Expression and Regulation of NaPi-IIa in a Murine Model Deficient for the Novel Interacting Partner GABARAP

Dissertation

zur

Erlangung der naturwissenschaftlichen Doktorwürde

(Dr. sc. nat.)

vorgelegt der

Mathematisch-naturwissenschaftlichen Fakultät

der

Universität Zürich

von

Sonja Reining

aus Deutschland

Promotionskomitee

Prof. Dr. Heini Murer (Vorsitz)

Dr. Nati Hernando (Leitung der Dissertation)

Prof. Dr. Jürg Biber

Prof. Dr. Florian Lang (Gutachter)

Zürich, 2009

INDEX

1. Summary

Renal reabsorption of inorganic phosphate (Pi) is mainly mediated by the Na-dependent Pi-cotransporter NaPi-IIa that is expressed in the brush border membrane (BBM) of renal proximal tubules. Regulation and apical expression of NaPi-IIa are known to depend on a network of interacting proteins. Most of the interacting partners identified so far associate with the C-terminal PDZ-binding motif (TRL) of NaPi-IIa. In a novel membrane yeast-two-hybrid (MYTH 2.0) screen of a mouse kidney library using the TRL-truncated cotransporter as bait, GABARAP was identified as a new interacting partner of NaPi-IIa.

GABARAP mRNA and protein are present in renal tubules and the interaction of NaPi-IIa and GABARAP was confirmed using GST-pull downs from BBM and co-immunoprecipitations from transfected HEK293 cells. Amino acids 36-68 of GABARAP were identified as a molecular determinant for the described interaction.

The *in vivo* effects of this interaction were studied in a murine model. GABARAP$^{-/-}$ mice have a reduced urinary excretion of Pi, a higher Na-dependent ^{32}Pi-uptake into renal BBMV, and an increased expression of NaPi-IIa in BBM as compared to GABARAP$^{+/+}$ mice. The expression of NHERF1, an important scaffold for the apical expression of NaPi-IIa, is also increased in GABARAP$^{-/-}$ mice.

Although baseline expression of NaPi-IIa is elevated, the absence of GABARAP does not interfere with the parathyroid hormone (PTH)-induced endocytosis of NaPi-IIa. Similarly, downregulation of NaPi-IIa induced by high content of Pi in the diet proceeds unaffected in GABARAP$^{-/-}$ mice. However, upregulation of the cotransporter in response to a chronic low Pi diet is greater in GABARAP$^{-/-}$ than in GABARAP$^{+/+}$ mice. Acute dietary regulation of NaPi-IIa is similar in GABARAP$^{-/-}$ and in GABARAP$^{+/+}$ mice.

In summary, GABARAP interacts with NaPi-IIa and controls the abundance of the cotransporter. Phosphaturic factors (PTH, high Pi diet) reduce the expression of NaPi-IIa to similar levels in GABARAP$^{-/-}$ and in GABARAP$^{+/+}$ mice, whereas NaPi-IIa expression is elevated in GABARAP$^{-/-}$ mice in the

absence of phosphaturic stimulus (normal diet) and under Pi conserving settings (low Pi diet). Therefore, we suggest that GABARAP exerts its effect on NaPi-IIa neither in the biosynthetic nor in the degradative pathway, but instead negatively influences NaPi-IIa basal turnover and/or half-life time *in vivo.*

2. Zusammenfassung

Die Reabsorption von anorganischem Phosphat (Pi) in der Niere wird hauptsächlich durch den Na-abhängigen Pi-Kotransporter NaPi-IIa vermittelt. Dieser ist in der Bürstensaummembran von proximalen Tubuluszellen exprimiert. Sowohl die Regulation als auch die Expression von NaPi-IIa in der apikalen Membran ist von einem Netzwerk von interagierenden Proteinen abhängig. Die meisten der bisher identifizierten Proteine dieses Netzwerks interagieren mit einer C-terminalen PDZ-bindenden Domäne (TRL) von NaPi-IIa. In einer neuen Hefe-zwei-Hybrid Durchsuchung mit einer C-terminalen Deletionsmutante (ΔTRL) von NaPi-IIa als Köderprotein wurde GABARAP als neuer interagierender Partner von NaPi-IIa identifiziert.

GABARAP mRNA sowie Protein sind in proximalen Tubuli exprimiert. Die Interaktion zwischen NaPi-IIa und GABARAP wurde sowohl durch „GST-pull down"-Experimente als auch mittels Ko-Immunpräzipitation verifiziert. Die Aminosäuren 36-64 von GABARAP stellen eine molekulare Determinante für die Interaktion dar.

Die Effekte dieser Interaktion konnten mittels eines GABARAP-defizienten Mausmodells *in vivo* untersucht werden. Im Vergleich zu $GABARAP^{+/+}$ Mäusen weisen $GABARAP^{-/-}$ Mäuse eine erniedrigte Pi-Exkretion im Urin, eine erhöhte Aufnahme von Pi in Bürstensaummembranvesikel sowie eine vermehrte Expression von NaPi-IIa in der renalen Bürstensaummembran auf. Zusätzlich wurde in $GABARAP^{-/-}$ Mäusen eine vermehrte Expression von NHERF1, eines wichtigen Ankerproteins für die apikale Lokalisation von NaPi-IIa, nachgewiesen.

Trotz der vermehrten Expression von NaPi-IIa unter normalen Bedingungen ist die durch das Parathormon induzierte Endozytose von NaPi-IIa in GABARAP-defizienten Mäusen nicht beeinträchtigt. Ebenso hat das Fehlen von GABARAP keinen Einfluss auf die Herunterregulation von NaPi-IIa durch eine chronisch verabreichte Pi-reiche Diät. Hingegen ist die Heraufregulation von NaPi-IIa als Antwort auf eine chronisch verabreichte Pi-arme Diät in $GABARAP^{-/-}$ Mäusen im Vergleich zu $GABARAP^{+/+}$ Mäusen verstärkt. Die akute Regulation von NaPi-IIa durch Pi-arme/Pi-reiche Diät

innerhalb weniger Stunden ist durch das Fehlen von GABARAP nicht beeinträchtigt.

Zusammenfassend lässt sich sagen, dass GABARAP mit NaPi-IIa interagiert und die apikale Expression des Kotransporters kontrolliert. Phosphaturische Faktoren (Pi-reiche Diät, Parathormon) erniedrigen die Expression von NaPi-IIa auf ein vergleichbares Niveau in GABARAP$^{-/-}$ und GABARAP$^{+/+}$ Mäusen. Im Gegensatz hierzu ist die Expression von NaPi-IIa in GABARAP$^{-/-}$ Mäusen in Abwesenheit phosphaturischer Faktoren (normale Diät) sowie unter phosphat-konservierenden Bedingungen (Pi-arme Diät) verstärkt. Diese Daten weisen darauf hin, dass GABARAP weder für den biosynthetischen noch für den degradierenden Pfad eine Rolle spielt. Stattdessen scheint GABARAP die stationäre Expression und/oder die Lebensdauer von NaPi-IIa in der Bürstensaummembran *in vivo* zu beeinflussen.

3. Introduction

3.1 The kidneys

The kidneys are bean-shaped organs that lie behind the peritoneum on each side of the vertebral column. Their main function is to regulate the electrolyte composition, acid-base balance and the volume of extracellular fluids. Furthermore, metabolic waste products and toxins are eliminated from the body by excretion in the urine. Although both kidneys together comprise to only ~0.5% of the body weight, they receive ~20% of the cardiac output. The blood enters the kidney via the renal artery and leaves the kidney through the renal vein after filtration. The urine exits the kidney through the ureters. The ureters from both kidneys empty into the bladder.

A cut section through the kidney reveals two basic layers: the granular cortex and an inner region called medulla (Fig.1). The granular appearance of the cortex is due to the presence of microscopic clusters of capillaries and convoluted epithelial tubules. In contrast to the cortex, tubules and blood vessels in the medulla are arranged in a parallel manner, resulting in a striated appearance.

Each human kidney consists of ~1 million nephrons, the functional subunits of the kidney. The blood is filtered through the endothelial wall of a tuft of capillaries that is called glomerulus. These capillaries are surrounded by podocytes which form a filtration barrier that allows filtration of water and small solutes but not of large molecules like proteins or even blood cells. The blood filtrate enters the nephron at the Bowman`s capsule which covers the glomerulus. From there, it passes through different subdivisions of the nephron and is converted into concentrated urine during its passage. From the Bowman`s space, the ultrafiltrate enters the proximal tubule. Based on its appearance, this division can be subdivided into the proximal convoluted tubule and the proximal straight tubule. The cells of the proximal tubule are characterized by an extensive amplification of both, the apical (luminal) and the basolateral (peritubular) membrane. Due to its infoldings, the apical membrane is also termed brush border membrane (BBM). The enlargement of the apical

surface area correlates with the main function of this nephron segment which is the reabsorption of the bulk of filtered fluid and solutes. The next subdivision of the nephron is the loop of Henle that is formed by the descending and ascending thin limbs and the thick ascending limb. The loop of Henle facilitates concentration of the urine due to a counterflow mechanism. The loop of Henle is followed by the distal convoluted tubule which terminates in the connecting tubule and finally in the collecting duct. These are the sites of fine control of salt and water excretion.

Two populations of nephrons can be distinguished. Superficial or cortical nephrons have only short loops of Henle. They account for the majority of nephrons and have mainly excretory and regulatory functions, whereas juxtamedullary nephrons with their long loops of Henle play a major role in concentration and dilution of the urine (Boron and Boulpaep 2005).

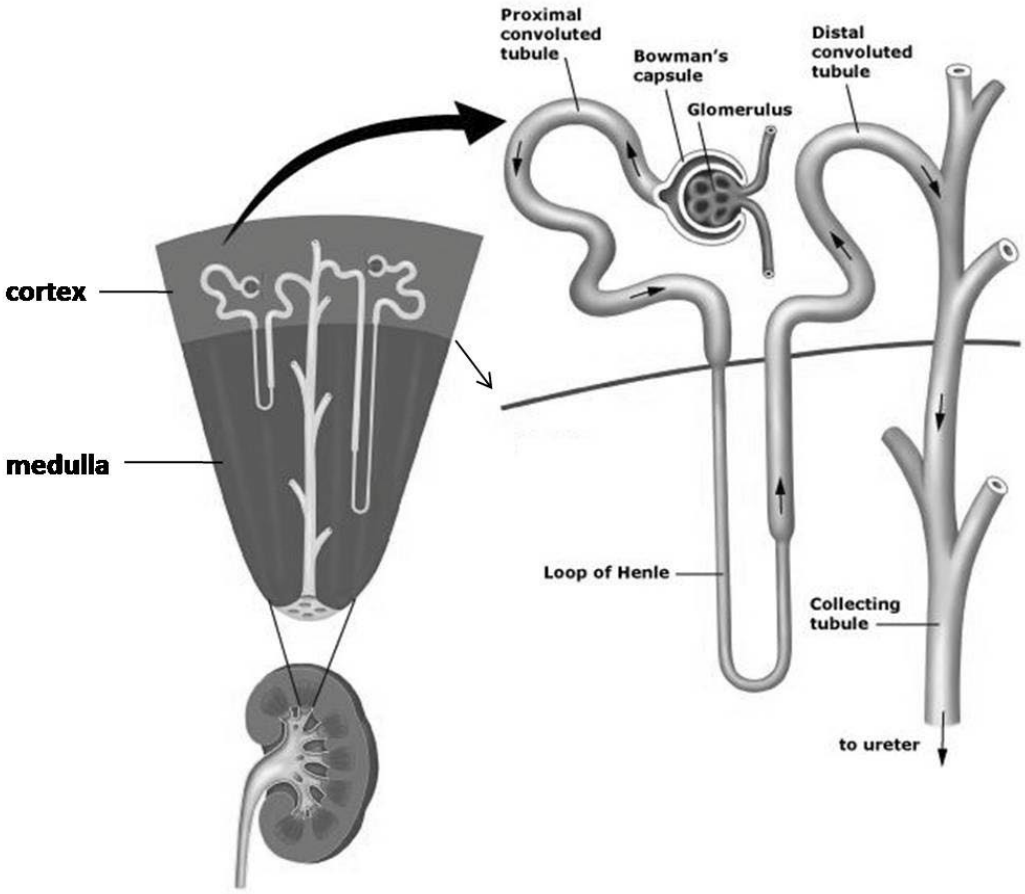

Figure 1: Anatomy of the kidney and the nephron.

(modified from www.uptodate.com)

3.2 Inorganic phosphate homeostasis

Inorganic phosphate plays an important role in a variety of cellular processes such as energy metabolism, nucleic acid synthesis, membrane function and bone mineralization. In addition, phosphorylation of proteins is a major regulatory mechanism involved in many cellular processes such as cell signaling and control of protein activity.

In the body, approximately 85% of the total phosphate is stored in the skeleton and teeth, whereas the remaining phosphate is distributed in soft tissues (14%) and in extracellular fluids (1%). Phosphate exists in two forms in the blood: in an organic form as phospholipids or phosphate esters and in the inorganic form - at the physiological blood pH 7.4 - mainly as divalent phosphate anion HPO_4^{2-}. The inorganic phosphate (Pi) accounts for ~30% of the total plasma phosphate. Of this Pi, only 85-90% can be freely filtered in the kidney whereas the remaining 10-15% is bound to proteins.

Because of its involvement in diverse biological processes and its limited solubility in the presence of divalent cations, the concentration of free Pi in extracellular as well as in intracellular compartments needs to be balanced in a millimolar range. Several organs are involved in Pi homeostasis. The daily need for Pi is covered by absorption of ~70% of the ingested Pi from the diet in the small intestine. The absorbed Pi is released into the blood and either deposited in the compartments described before or filtered in the kidney. Renal Pi excretion can be adjusted in a tight and rapid manner to hormones and metabolic factors that influence Pi homeostasis. In contrast, intestinal absorption is adjusted rather slowly and is believed to play only a minor role in the control of Pi homeostasis. In a situation of neutral Pi balance, the amount of Pi that is absorbed in the small intestine equals the amount of Pi that is excreted in the urine. Under physiological conditions, 80-90% of the Pi that is filtered in the glomeruli is reabsorbed in the renal proximal tubules.

The proximal tubule reabsorbs Pi by the transcellular route. The rate-limiting step occurs at the apical membrane of the proximal tubular cells, which is the site for a secondary active transport process. In this transport process the electrochemical sodium gradient is utilized to mediate uphill transport of Pi into proximal tubular cells. In contrast to the apical entry of Pi into the cells, the basolateral exit of Pi remains poorly understood.

3.3 Phosphate transporters

Several mammalian phosphate transporters have been identified and characterized at the molecular level. These phosphate transporters have been grouped into three different protein families: type I, type II and type III. According to the human genome database (http://www.gene.ucl.ac.uk/nomenclature) the transporters are assigned to the solute carrier series SCL17, SLC34 and SLC20.

3.3.1 Type I NaPi cotransporters (SLC17)

Type I NaPi cotransporters are expressed in the kidney, liver and brain. Within the kidney, the type I NaPi cotransporter is localized in the brush-border membrane of proximal tubules (Biber, Custer et al. 1993). Expression in *Xenopus laevis* oocytes revealed that the type I NaPi cotransporter mediates sodium-dependent transport of Pi at high extracellular Pi concentrations. However, in addition to Pi, the type I NaPi-cotransporter transports a variety of other anions and might also possess chloride channel activity (Busch, Schuster et al. 1996). The type I NaPi cotransporter is not regulated by factors that are known to influence renal Pi reabsorption (Werner, Dehmelt et al. 1998). Interestingly, a type I related NaPi cotransporter is likely to be involved in vesicular glutamate uptake in the brain (Bellocchio, Reimer et al. 2000).

3.3.2 Type II NaPi cotransporters (SLC34)

The SLC34 family comprises three members: NaPi-IIa, NaPi-IIb and NaPi-IIc. Type II NaPi cotransporters are expressed in several epithelial tissues. In the kidney (NaPi-IIa and NaPi-IIc) and in the small intestine (NaPi-IIb), these transporters are located in apical membranes and represent the rate-limiting step of transepithelial Pi transport (Murer, Forster et al. 2004) (Fig. 2). Unlike type I NaPi cotransporters, members of the type II NaPi family mediate exclusively Pi transport and this transport is strictly sodium-dependent. Due to their different Na^+:Pi stoichiometry, the Pi transport by NaPi-IIa and NaPi-IIb is

electrogenic whereas NaPi-IIc is electroneutral. The abundance of type II NaPi cotransporters is controlled by factors that influence Pi homeostasis.

NaPi-IIa is expressed primarily in renal proximal tubules, where it is localized in microvilli that form the brush border membrane. In addition, expression of NaPi-IIa is also found in bone cells and neurons (Gupta, Guo et al. 1997; Hisano, Haga et al. 1997). Within the kidney, NaPi-IIa expression is restricted to the brush border membrane of proximal tubules. Under standard dietary conditions, NaPi-IIa expression is highest in proximal convoluted tubules (S1, S2) and gradually decreased towards the end of the proximal straight tubule (S3). Expression of NaPi-IIa is more pronounced in juxtamedullary than in superficial nephrons (Custer, Lotscher et al. 1994). Thus, NaPi-IIa expression in the kidney matches with the main sites of renal Pi reabsorption.

NaPi-IIb expression has been described in the small intestine and other organs such as lung, liver and mammary glands. In the small intestine, NaPi-IIb is localized in the brush border membrane of enterocytes and mediates Pi absorption from the diet (Hilfiker, Hattenhauer et al. 1998).

NaPi-IIc expression is found exclusively in renal proximal tubules. It has been described to be a growth-related transporter with a higher expression in weaning mice and a progressive decrease with age (Segawa, Kaneko et al. 2002). However, young NaPi-IIc$^{-/-}$ mice show hypercalciuira and hypercalcemia but not hypophosphatemia. Furthermore, renal NaPi cotransport activity and urinary Pi excretion is not affected by the loss of NaPi-IIc (Segawa, Onitsuka et al. 2009).

Based on the severe renal Pi wasting phenotype of NaPi-IIa$^{-/-}$ mice (Beck, Karaplis et al. 1998), it has been proposed that NaPi-IIa is the major Pi transporter in the adult murine kidney, whereas NaPi-IIc was considered to playing only a minor role. However, mutations of NaPi-IIc identified in families with several hypophosphatemic syndromes and in particular the detectable phenotype in the heterozygotes (Bergwitz, Roslin et al. 2006; Ichikawa, Sorenson et al. 2006; Lorenz-Depiereux, Benet-Pages et al. 2006) points to either dramatic differences between humans and mice or an incomplete understanding of renal handling of Pi.

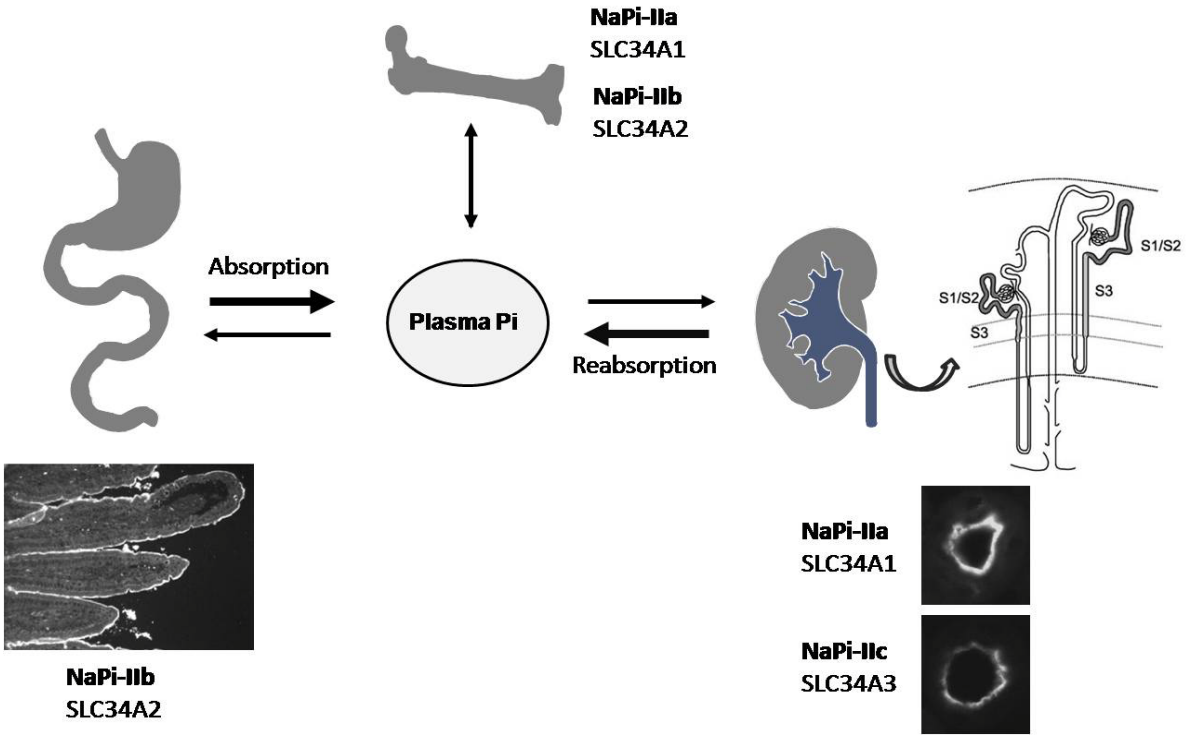

Figure 2: SLC34 transporters and Pi homeostasis.

3.3.3 Type III NaPi cotransporters (SLC20)

The most recent family of NaPi cotransporters that has been described is the SLC20 family (Collins, Bai et al. 2004). Their members were originally identified as retroviral receptors. Later it has been shown that both receptors of this family (now renamed into PiT-1 and PiT-2) induce Pi transport in a sodium-dependent manner after expression in *Xenopus laevis* oocytes (Kavanaugh, Miller et al. 1994). Both proteins are almost ubiquitously expressed in rat tissues. Interestingly, PiT-2 related mRNA expression increases in response to incubation of cells in Pi-free medium (Chien, O'Neill et al. 1998). Recent findings suggest that PiT-2 might contribute to renal Pi reabsorption based on its localization in the brush border membrane in proximal tubules (Villa-Bellosta R., Ravera S., in press). Its precise physiological role for Pi homeostasis remains to be established.

3.4 NaPi-IIa

Knock-out of the gene encoding for NaPi-IIa (Npt2) led to the conclusion that the bulk of Pi is reabsorbed by this cotransporter. Pi transport into brush border membrane vesicles isolated from NaPi-IIa$^{-/-}$ mice was reduced by 70%, consistent with the hypophosphatemic state of these animals (Beck, Karaplis et al. 1998). The remaining 30% of NaPi-transport activity was attributed to the maximally increased expression of NaPi-IIc (Tenenhouse, Martel et al. 2003). As described in the above section, also other Pi-transporters, such as PiT-2, might contribute to the remaining transport activity in NaPi-IIa$^{-/-}$ mice. However, these findings suggest that in adult wild-type mice, renal Pi reabsorption is largely determined by the transport activity of NaPi-IIa.

3.4.1 General characteristics

NaPi-IIa consists of 635 amino acids (Magagnin, Werner et al. 1993) and migrates with an apparent molecular weight of 80-90 kDa in SDS-gels under non-reducing conditions. Based on data obtained from cysteine scanning, hydropathy analysis and epitope tagging studies a structural model of NaPi-IIa has been proposed (Fig. 3). According to this model, NaPi-IIa has eight transmembrane domains with both, the N- and the C-terminus facing the intracellular compartment. A large extracellular domain (ECL2) contains two N-glycosylation sites. Furthermore, this domain links two halves of the protein that contain conserved repeated sequences. These repeated motifs may form two opposed reentrant loops which then constitute the Pi transport pathway (Biber, Hernando et al. 2008).

The preferred substrate of NaPi-IIa is divalent Pi. Due to the transport stoichiometry of three Na^+ and one HPO_4^{2-} ions, NaPi-IIa is an electrogenic cotransporter that transports one net positive charge per cycle into the cell. The binding order of Na^+ and HPO_4^{2-} ions has been revealed. The transport cycle is initiated by the binding of one Na^+, followed by binding of the HPO_4^{2-} and subsequent binding of two Na^+ ions (Forster, Loo et al. 1999). Protons can interact with the empty transporter and also with the final Na^+ binding steps. Therefore, NaPi-IIa cotransport is pH-dependent with higher transport rates at more basic external pH values (Forster, Kohler et al. 2002).

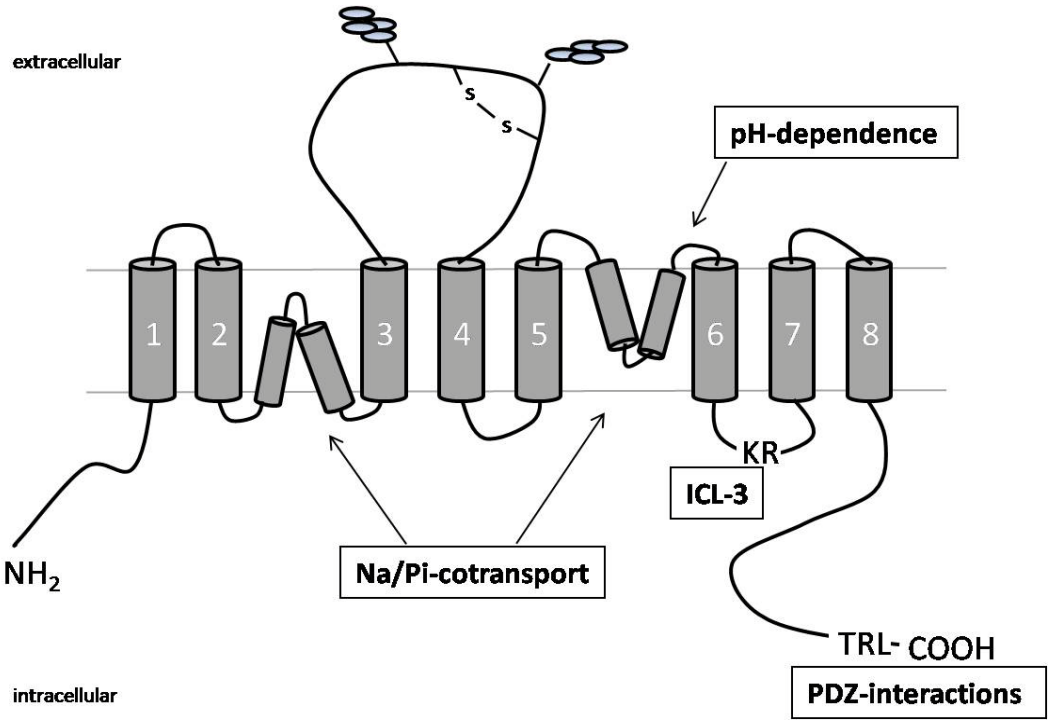

Figure 3: Proposed structural model of NaPi-IIa.

3.4.2 Regulation of NaPi-IIa

Pi homeostasis is mainly controlled by adjustments of Pi reabsorption in the kidney. Many hormones and metabolic factors operate primarily on this step. Theoretically, Pi reabsorption in renal proximal tubules could be adjusted by three different mechanisms: changing the abundance of the transporter, alterations of the apparent affinities for the substrates or changes of the lipid composition which may influence the preferred protein conformation and thus influence transport activity. Pi reabsorption via NaPi-IIa is controlled by adjusting the amount of transporters that reside in the brush border membrane rather than changing their intrinsic transport activity. On the one hand, membrane abundance of NaPi-IIa depends on the biosynthetic pathway and membrane insertion. On the other hand, NaPi-IIa downregulation occurs by endocytotic membrane retrieval. Endocytosed NaPi-IIa proteins are degraded in lysosomes with no or little recycling back to the membrane (Keusch, Traebert et al. 1998).

Several Pi wasting disorders have been described that involve changes of the expression of NaPi-IIa. These are the inherited disorders X-linked hypophosphatemia (XLX), autosomal dominant hypophosphatemic rickets (ADHR) and the acquired disorder oncogenic hypophosphatemic osteomalacia (OHO). Studies related to these disorders revealed the importance of two genes, PHEX and FGF23, for NaPi-IIa expression (Fukumoto and Yamashita 2002; Tenenhouse and Sabbagh 2002) (Fig. 4). The PHEX gene encodes a protein that is a member of a family of membrane-bound metalloproteases. It has been postulated that PHEX plays a role in the activation or inactivation of peptide factors involved in the regulation of renal Pi reabsorption (Takeda, Yamamoto et al. 2004). FGF23 might be a substrate of this metalloprotease and thus accumulates when the PHEX gene harbors inactivating mutations. Elevated serum levels of FGF23 lead to a decreased NaPi-IIa abundance and Pi wasting. As expected, the opposite effect (increased Pi reabsorption) was found in $FGF23^{-/-}$ mice (Shimada, Kakitani et al. 2004). It has been shown that FGF23 might be involved in dietary regulation of Pi reabsorption. FGF23 controls the effect of the diet on NaPi-IIa independently on changes of other phosphaturic hormones, such as PTH, in the blood plasma (Segawa, Kawakami et al. 2003).

Interestingly, knock-out of a gene encoding for a type I membrane protein named Klotho results in a phenotype that has striking similarities to the one observed in $FGF23^{-/-}$ mice (Razzaque 2008). Hyperphosphatemia in $klotho^{-/-}$ mice correlates with increased levels of NaPi-IIa and NaPi-IIc (Segawa, Yamanaka et al. 2007). In addition, $klotho^{-/-}$ mice have highly elevated serum FGF23 levels, possibly due to an end-organ resistance to FGF23 and a positive feedback-loop (Stubbs, Liu et al. 2007). Studies have shown that Klotho acts as a cofactor which allows FGF23 to bind to its receptor complex with much higher affinity than to FGFR alone and therefore facilitates subsequent signaling activities of the receptor (Kurosu, Ogawa et al. 2006; Goetz, Beenken et al. 2007; Medici, Razzaque et al. 2008).

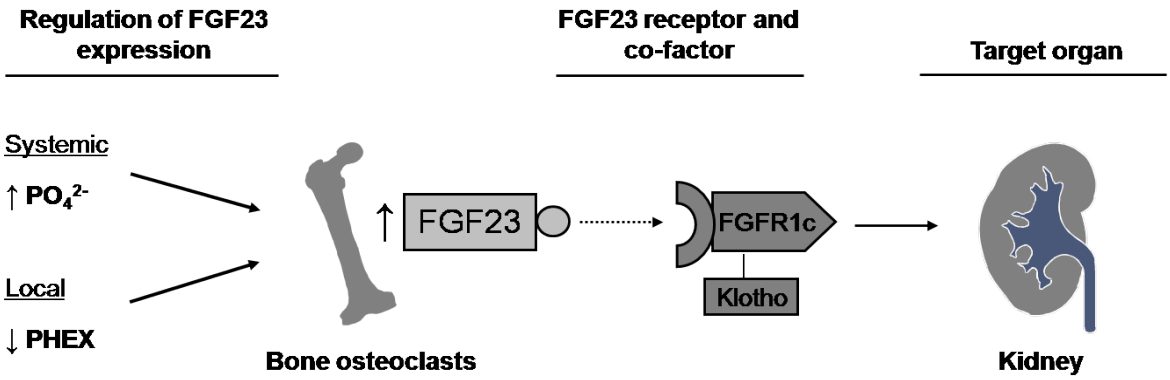

Figure 4: The phosphaturic hormone FGF23.

(modified from Stubbs et al., Seminars in Dialysis-Vol. 20, 2007)

3.4.2.1 Dietary Phosphate

One factor that controls NaPi-IIa membrane expression and thus renal tubular reabsorption of Pi is the dietary Pi intake, with high Pi diet decreasing and low Pi diet increasing the expression of NaPi-IIa in the proximal microvilli (Fig. 5). Upregulation of NaP-IIa upon intake of a low Pi diet results in the presence of NaPi-IIa in superficial nephrons which, as mentioned before, express very little amounts of the cotransporter in normal dietary conditions. Adaptation in response to dietary Pi content can be observed within less than one hour (acute adaptation) and remains stable even during prolonged dietary administration (chronic adaptation).

Acute changes are independent on transcriptional regulation of NaPi-IIa, whereas the situation for the chronic adaptation is not that clear. In weaning mice chronically fed with a low Pi diet NaPi-IIa protein increase is paralleled by an increase of its mRNA (Kido, Miyamoto et al. 1999), whereas in adult mice no such transcriptional regulation could be observed after chronic feeding with a low Pi diet (Madjdpour, Bacic et al. 2004).

Acute increase of NaPi-IIa protein in the apical membrane in response to a low dietary Pi content is independent on *de novo* protein synthesis since it could not be blocked by cycloheximide, an inhibitor of translational elongation in eukaryotic organisms (Levine, Ho et al. 1986). This observation could be explained by the translocation of a subapical pool of NaPi-IIa cotransporters into

the apical membrane. However, the existence of such an intracellular pool of NaPi-IIa cotransporters is not proven.

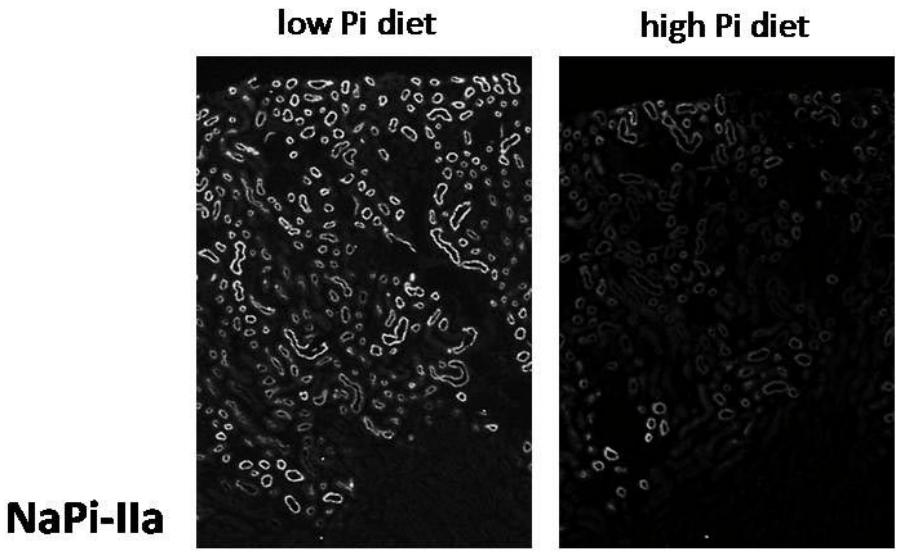

Figure 5: Dietary regulation of NaPi-IIa in mice fed with a low or a high Pi diet for five days.

Opposed to the effect of a low Pi diet, intake of a high dietary Pi content leads to a decrease of NaPi-IIa membrane abundance and an increase of urinary Pi excretion. Also this adaptation occurs in a rapid way and is completed within four hours after intake of a high Pi diet (Capuano, Bacic et al. 2005). The internalized NaPi-IIa undergoes lysosomal degradation.

In addition to NaPi-IIa, also NaPi-IIc is regulated by dietary Pi intake. However, the mechanisms seem to differ from those involved in NaPi-IIa regulation. Acute regulation of NaPi-IIc is not observed (Segawa, Yamanaka et al. 2005) and chronic regulation of NaPi-IIc involves transcriptional changes (Madjdpour, Bacic et al. 2004).

3.4.2.2 PTH

The parathyroid hormone (PTH) is one of the best understood humoral factors which control the apical expression of NaPi-IIa (Fig. 6). PTH is a potent phosphaturic hormone that causes rapid internalization of NaPi-IIa via the

pathway of receptor-mediated endocytosis. Internalization occurs at the microvillar clefts, possibly in clathrin-coated vesicles (Bacic, Lehir et al. 2006). As mentioned before, morphological and biochemical data point to a subsequent lysosomal degradation of NaPi-IIa (Keusch, Traebert et al. 1998). PTH-induced downregulation of NaPi-IIa is independent on transcriptional changes.

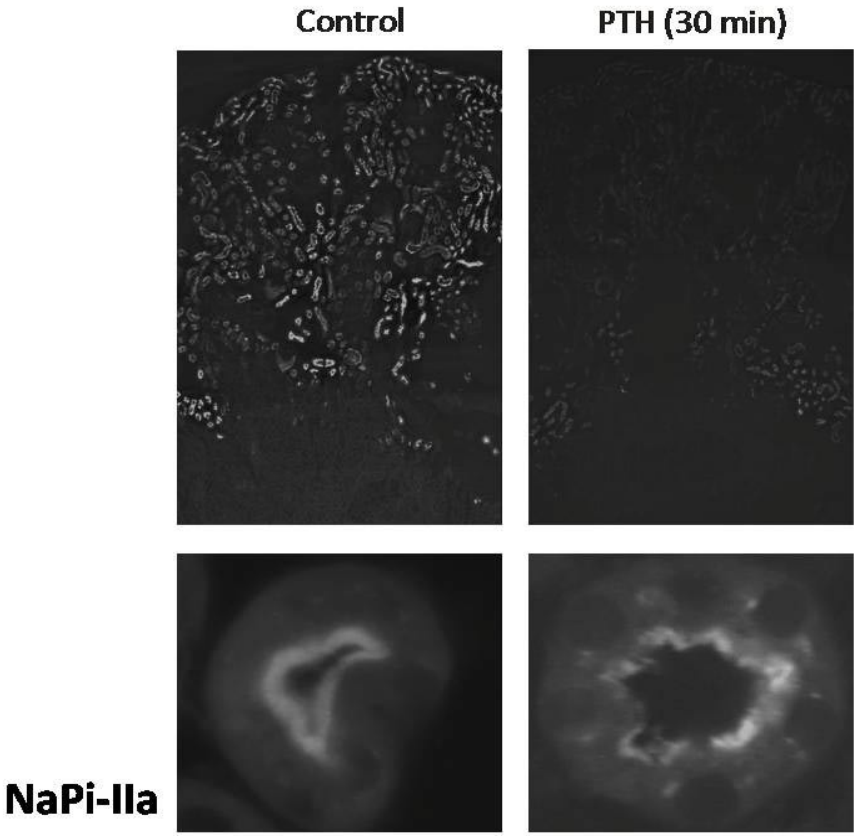

Figure 6: PTH-induced downregulation of NaPi-IIa.

(modified from Capuano et al., Am J Physiol Cell Physiol. Vol. 292, 2007)

The signaling events that lead to membrane retrieval of NaPi-IIa cotransporters have been studied in great detail (Fig. 7). PTH-receptors are G-protein coupled receptors which are localized on the apical as well as on the basolateral membrane of renal proximal tubular cells. However, their intracellular signaling pathways are not identical due to their coupling to different subfamilies of G-proteins (Traebert, Volkl et al. 2000). The apical PTH-receptor activates preferentially the phospholipase C (PLC)/ protein kinase C

(PKC) pathway. Although this PLC activation has been considered to involve G_q-proteins, recent data suggest the implication of the $G_{i/o}$ subfamily (see 3.5.1). In contrast, the basolateral PTH-receptor is linked to the subfamily of G_s-proteins. G_s-proteins activate the adenylyl cyclase (AC). Generation of the second messenger cAMP leads to activation of the protein kinase A (PKA). Despite this difference in the initial PTH-induced signaling, both pathways partially converge at the level of the MAP-kinases ERK1/2. Pharmacological inhibition of ERK1/2 activation impairs the PTH-induced NaPi-IIa internalization in kidney slices (Bacic, Schulz et al. 2003).

The molecular link between ERK1/2 activation and endocytosis of NaPi-IIa is not yet understood. To date, there is no convincing evidence for a phosphorylation of NaPi-IIa itself. Instead, phosphorylation is believed to play a role on the level of NaPi-IIa interacting proteins which are required for its localization and regulation (see 3.5.1).

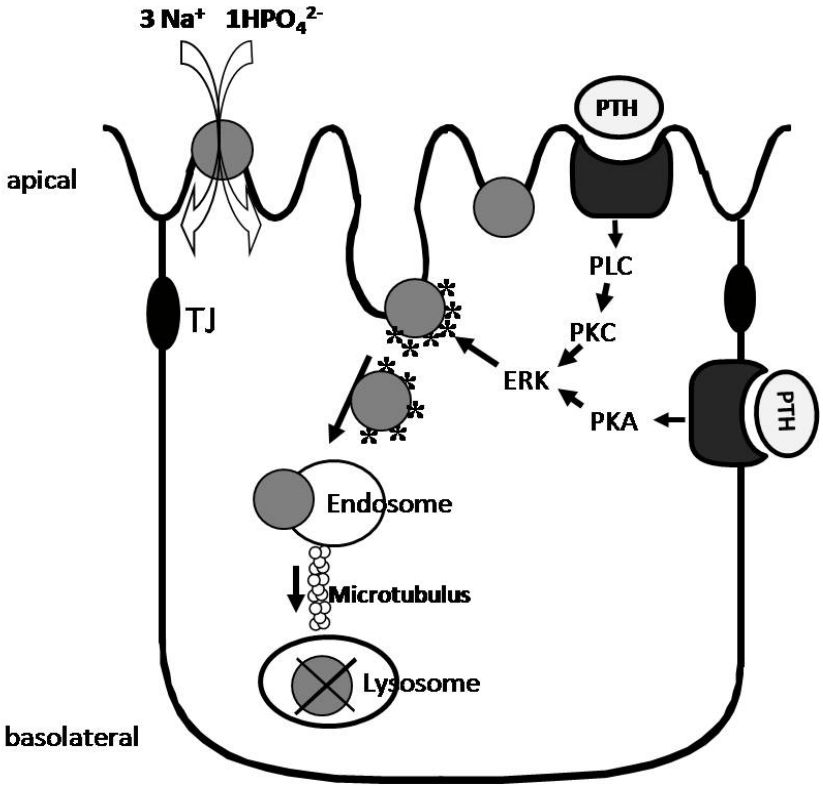

Figure 7: Signaling events leading to the PTH-induced internalization of NaPi-IIa.

Interestingly, PTH does not induce internalization of NaPi-IIb. This insensitivity of NaPi-IIb enabled the identification of the molecular domains of NaPi-IIa that are required for its PTH-induced downregulation. Chimeras of NaPi-IIa and NaPi-IIb were tested for their PTH-responsiveness. These studies led to the identification of a dibasic KR-motif within the third intracellular loop which is strictly required for the PTH-induced endocytosis of NaPi-IIa (Karim-Jimenez, Hernando et al. 2000).

3.5 NaPi-IIa interacting proteins

The localization of NaPi-IIa in the apical brush border membrane and its controlled expression is believed to depend on a network of interacting proteins. Theoretically, these interacting proteins could either regulate the trafficking of NaPi-IIa to the apical membrane, they could act as scaffolding proteins to stabilize NaPi-IIa in the membrane or they could be required for the correct organization of the signaling complexes that lead to internalization of the cotransporter. The latter mechanism has been described for the PKA-mediated regulation and internalization of the sodium-proton exchanger NHE3, a transport protein that is also localized in apical brush border membranes of renal proximal tubules (Weinman, Steplock et al. 2003).

Different yeast-two-hybrid screens were performed to identify such interacting partners of NaPi-IIa (Fig. 8). In one of them, the PTH-responsive third intracellular loop of NaPi-IIa was used as bait. PEX19, a human peroxisomal farnesylated protein was identified as a NaPi-IIa interacting protein in this screen. The interaction with PEX19 depends on the presence of the KR motif of NaPi-IIa. Overexpression of PEX19 has been shown to induce internalization of NaPi-IIa in OK cells (Ito, Iidawa et al. 2004), a cell line obtained from opossum kidney that retaines properties of proximal epithelia.

Another yeast-two-hybrid screen was performed using the N-terminal domain of NaPi-IIa as bait. Results obtained from this screen suggested that MAP17, a small membrane-associated protein interacts with the N-terminus of NaPi-IIa. Interestingly, MAP17 additionally interacts with the PSD-95/Drosophila discs large/ZO-1 (PDZ)-domain containing protein PDZK1. PDZK1 interacts

also with the C-terminus of NaPi-IIa directly (see later). The physiological role of the interaction between NaPi-IIa and MAP17 has been studied with somewhat conflicting results. An earlier study reported that MAP17 is required for apical positioning of PDZK1 based on co-expression of both interacting proteins in OK cells (Pribanic, Gisler et al. 2003). In contrast to this observation, other investigators suggest that co-expression of MAP17 and PDZK1 in OK cells leads to a translocation of the whole MAP17/PDZK1/NaPi-IIa complex to the trans-Golgi network in a PKC-dependent manner (Lanaspa, Giral et al. 2007). However, it has been shown that PTH-induced activation of PKC in mice did not induce a change in localization of MAP17 or PDZK1 (Pribanic, Gisler et al. 2003). Thus, the precise role of MAP17 in the regulation of NaPi-IIa is still not understood.

The last three amino acids at the C-terminus of NaPi-IIa (TRL) constitute a PDZ-binding motif. Apical expression of NaPi-IIa depends on the presence of this motif as illustrated by the observation that a ΔTRL cotransporter partially accumulates intracellularly (Karim-Jimenez, Hernando et al. 2001). Yeast-two-hybrid analysis with the C-terminal domain as bait led to the identification of numerous PDZ-domain containing proteins as potential NaPi-IIa interacting partners (Gisler, Stagljar et al. 2001). Interestingly, all four members of the sodium-hydrogen exchanger regulatory factor (NHERF)-family (NHERF1-4) were identified as interacting proteins in this screen (Gisler, Stagljar et al. 2001). These four PDZ-proteins are expressed in or in close proximity to the proximal brush border membrane. The impact on NaPi-IIa expression and regulation has been studied in knock-out mouse models for two members of the NHERF-family recently (see 3.5.1 and 3.5.2). In addition, expression in renal proximal tubules and co-localization with NaPi-IIa has been confirmed for some other PDZ-proteins also identified in this (and other) yeast-two-hybrid screening. These include MAST205 (a 205 kDa microtubule-associated serine/threonine kinase), CAL (CFTR-associated ligand), PDZ-RGS3 (PDZ-containing regulator of G-protein coupled signaling 3), (S. Reining, unpublished observations) and Shank2E (SH3/ankyrin domain gene 2; splice variant E). The latter has been shown to undergo Pi-induced internalization similar to NaPi-IIa (McWilliams, Breusegem et al. 2005).

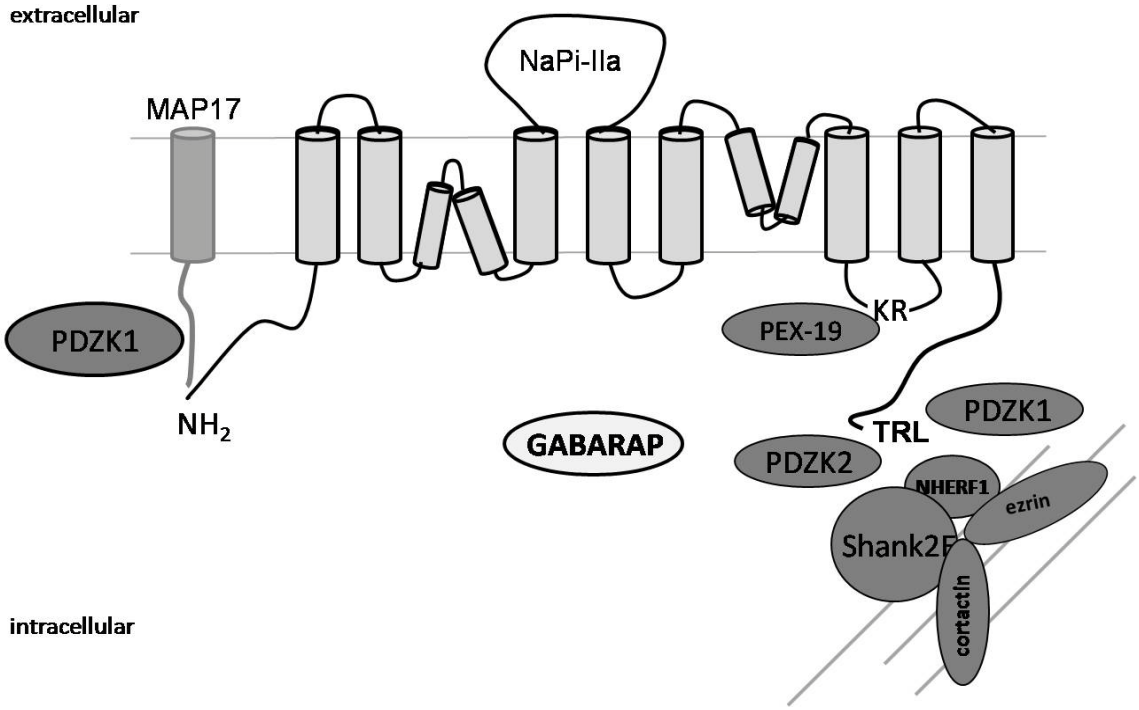

Figure 8: Summary of NaPi-IIa interacting proteins.

3.5.1 NHERF1

NHERF1 is a 50 kDa protein that is associated with the apical membrane of renal epithelial cells. It was first identified as a crucial adaptor component in a multiprotein complex that is required for PKA phosphorylation and inactivation of the sodium hydrogen exchanger NHE3 (Weinman, Minkoff et al. 2000). It is characterized by two tandem PDZ-domains and a C-terminal moesin-ezrin-radixin-merlin (MERM)-binding domain. The first PDZ-domain mediates the interaction between NHERF1 and NaPi-IIa. The MERM-binding domain interacts with proteins of the MERM family, such as ezrin, and thus may link NaPi-IIa to the actin cytoskeleton (Reczek, Berryman et al. 1997). Ezrin also functions as an A kinase anchoring protein (AKAP) due to its ability to bind to the regulatory subunit of PKA.

Disruption of the interaction between NaPi-IIa and NHERF1 leads to a reduced apical expression of NaPi-IIa in cells (Hernando, Deliot et al. 2002). Moreover, apical expression of NaPi-IIa is reduced in NHERF1$^{-/-}$ mice and the

cotransporter accumulates in intracellular vesicles. This is consistent with the mild renal Pi wasting phenotype that was observed in these animals (Shenolikar, Voltz et al. 2002). Surprisingly, NHE3 abundance in the apical membrane was not affected by the loss of NHERF1, suggesting that NHERF1 is important for apical positioning of some but not all interacting membrane proteins. Upregulation of NaPi-IIa in response to a low Pi diet is impaired in NHERF1$^{-/-}$ mice, a finding which is in line with a role of NHERF1 in apical scaffolding of NaPi-IIa (Weinman, Boddeti et al. 2003).

In addition to its function as scaffolding protein, NHERF1 also plays an important role for the signaling cascade that leads to PTH-induced downregulation of NaPi-IIa. This is due to its ability to interact simultaneously with type I PTH-receptors (PTH1R) and PLCβ in a PDZ-dependent way. In most cells, PTH1R couples to G_s- or G_q-proteins. Coupling to G_s leads to an increase of adenylyl cyclase activity and a rise in cAMP which in turn activates PKA whereas coupling to G_q results in activation of PLC/PKC. However, *in vitro* studies with NHERF2, a protein with very similar properties to NHERF1, demonstrated that PTH couples to $G_{i/o}$-proteins when the PTH1R is bound to NHERF2. This particular subfamily of inhibitory G-proteins signal via activation of PLCβ (by the βγ-subunits of the G-protein) and inhibition of adenylyl cyclase (by the α-subunit) (Mahon, Donowitz et al. 2002). Since NHERF1 is only present at the apical membrane, the described reaction could take place on the apical but not on the basolateral membrane. This would explain why signaling of basolateral PTH-receptors occurs via activation of PKA whereas the apical PTH-response is shifted towards PKC activation in renal proximal tubules (Fig. 3). Indeed it has been shown that stimulation of only apical PTH-receptors failed to induce internalization of NaPi-IIa in NHERF1$^{-/-}$ mice (Capuano, Bacic et al. 2007).

Interestingly, activation of PKC and PKA leads to phosphorylation of NHERF1 itself and PTH causes a dissociation of the NaPi-IIa/NHERF1 complex in OK cells and murine kidney (Deliot, Hernando et al. 2005). In a recent publication, a serine residue located within the first PDZ-domain of NHERF1 has been shown to be phosphorylated upon PKC and PKA activation. It has been proposed that phosphorylation of this residue may change the conformation of the whole PDZ-domain and thus reduces the binding affinity of

NHERF1 for NaPi-IIa (Weinman, Biswas et al. 2007). The “released” NaPi-IIa could be then internalized according to this model.

In summary, NHERF1 is an important scaffolding protein that anchors NaPi-IIa in the apical membrane. Additionally, it also influences signaling events which lead to a membrane retrieval of NaPi-IIa.

3.5.2 PDZK1

PDZK1 (NHERF3) is a protein that consists of ~520 amino acids which form four tandem PDZ-domains. It is expressed in epithelial cells of the kidney, pancreas, liver, gastrointestinal tract and adrenal cortex (Kocher, Comella et al. 1998). Renal expression is restricted to the proximal tubule where PDZK1 co-localizes with NaPi-IIa in the brush border membrane.

The C-terminal TRL-motif of NaPi-IIa has been shown to interact specifically with the third PDZ-domain of PDZK1 (Gisler, Pribanic et al. 2003). The fourth PDZ-domain of PDZK1 interacts with NHERF1. It has been suggested that PDZK1 is part of a network of proteins which are involved in trafficking, apical positioning and regulation of various transporters, receptors and components of signaling cascades (Gisler, Madjdpour et al. 2003; Gisler, Pribanic et al. 2003). Knock-out of PDZK1 did not impair renal Pi handling and NaPi-IIa membrane expression under normal dietary conditions. Acute dietary regulation as well as PTH-induced downregulation of NaPi-IIa was similar in PDZK1$^{-/-}$ compared to PDZK1$^{+/+}$ mice. Only chronic feeding of PDZK1$^{-/-}$ mice with a high Pi diet reduced NaPi-IIa abundance in the apical membrane and increased urinary Pi excretion even further compared to PDZK1$^{+/+}$ mice (Capuano, Bacic et al. 2005). The lack of a prominent phenotype for NaPi-IIa in PDZK1$^{-/-}$ mice could be due to compensation by other PDZ-proteins such as the closely related PDZK2 (NHERF4). Similar to PDZK1, PDZK2 consists of four PDZ-domains and is expressed in renal proximal tubules. Pull-down analysis and co-immunoprecipitation confirmed the interaction between NaPi-IIa and PDZK2. The C-terminal TRL-motif of NaPi-IIa and the third PDZ-domain of PDZK2 are the required molecular determinants for the interaction (S. Reining,

unpublished results). The precise physiological roles of PDZK1 and PDZK2 in the context of Pi homeostasis remain to be clarified.

3.6 Advantage of a novel membrane yeast-two-hybrid system

Classical yeast-two hybrid screenings relay on the reconstitution of transcription factor activity upon interaction between bait and prey. Therefore, it depends on nuclear transport of both bait and prey constructs. In practical terms this excludes the possibility to use full-length membrane proteins as bait. Indeed the three screenings mentioned above were performed using discrete intracellular domains of NaPi-IIa (N-terminus, third intracellular loop, C-terminus) as bait.

More recently, a new yeast-two-hybrid approach has been developed allowing to studying interactions of full-length membrane proteins. This approach depends on the reconstitution of ubiquitin which is split in two halves (Fig. 9). One of the halves is fused to the bait whereas the other halve is fused to the prey. Upon bait-prey interaction, the two halves of ubiquitin are brought together and the transcription factor that is fused to the membrane protein of interest (bait) is cleaved and released by ubiquitin specific proteases. The free transcription factor enters the nucleus and activates the transcription of reporter genes (Gisler, Kittanakom et al. 2008).

This new method was applied to search for additional NaPi-IIa interacting partners. In order to prevent PDZ-based interactions, a ΔTRL (instead of the full-length) NaPi-IIa construct was used as bait. This membrane yeast-two-hybrid screening led to the identification of GABARAP as a new interacting partner of NaPi-IIa.

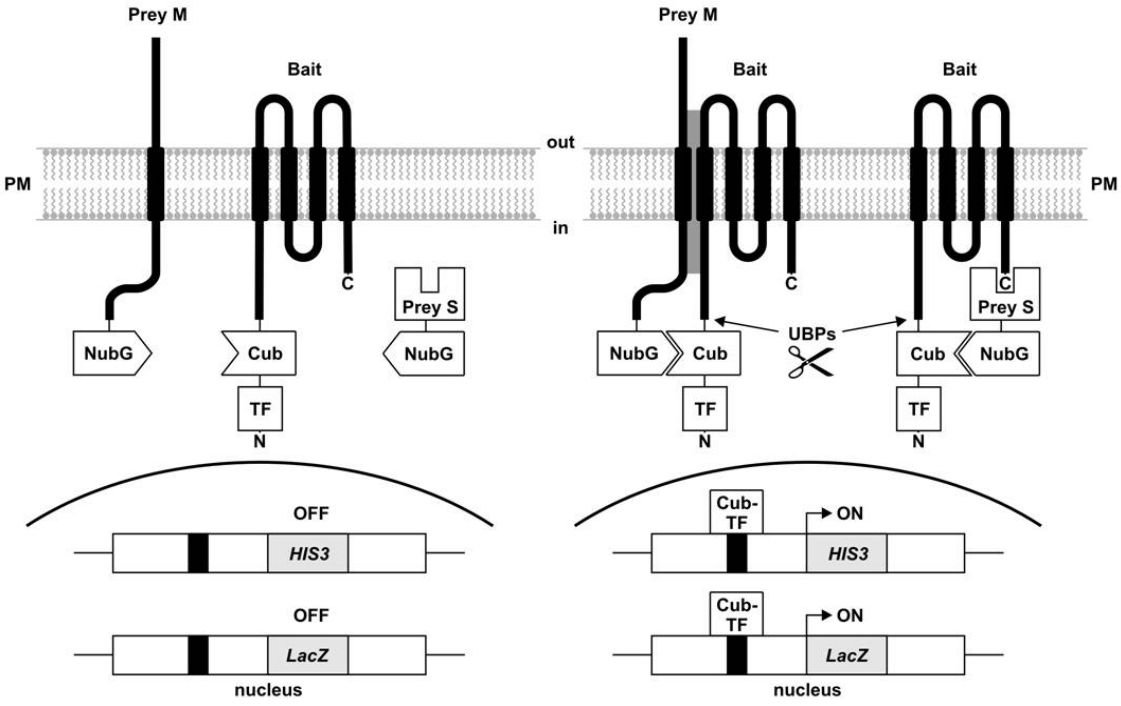

Figure 9: Principle of the membrane yeast-two-hybrid screen.

PM: plasma membrane; NubG: N-terminal half of the split ubiquitin containing a mutation from isoleucine to glycine which prevents self-reconstitution; Cub: C-terminal half of split-ubiquitin TF: transcription factor; UBPs: ubiquitin specific protases
(modified from Gisler et al., Mol Cell Proteomics. Vol. 7, 2008)

3.7 GABARAP

GABARAP was originally identified as a $GABA_A$-Receptor Associated Protein (Wang, Bedford et al. 1999). It has been shown later that expression of GABARAP is not restricted to the brain. Thus, GABARAP protein is also detected in kidney, liver, spleen, skeletal muscle and heart (Tanida, Ueno et al. 2004) as well as in various human cell lines (Green, O'Hare et al. 2002). Regarding the subcellular localization of GABARAP, a punctate distribution within the cytoplasm has been reported in some breast epithelial cells, HeLa cells and neurons (Wang, Bedford et al. 1999; Kneussel, Haverkamp et al. 2000; Green, O'Hare et al. 2002; Klebig, Seitz et al. 2005).

Interestingly, GABARAP belongs to a family of proteins which are evolutionary highly conserved among eukaryotic species from yeast over plants to mammals (Coyle and Nikolov 2003). The sequence identity between human GABARAP and its mouse orthologue is 100%. In addition, several GABARAP-

like homologues have been identified in human and in mouse (Sagiv, Legesse-Miller et al. 2000; Vernier-Magnin, Muller et al. 2001; Xin, Yu et al. 2001), suggesting a critical function of this protein family.

The GABARAP protein consists of 117 amino acids and has an asymmetric structure with a basic N-terminal region and an acidic C-terminus (Fig. 10). Amino acids 1-22 at the N-terminus potentially form an α-helix with five positively charged amino acids on one side of the helix. This motif has been shown to interact with tubulin and to promote tubulin assembly *in vitro* (Wang and Olsen 2000). The amino acids between residue 36 and 68 have been shown to mediate the interaction with the γ-subunit of $GABA_A$-receptors (Wang, Bedford et al. 1999). In addition, GABARAP interacts with a variety of other receptors among them the transferrin receptor (Green, O'Hare et al. 2002) and the angiotensin II type 1 receptor (Cook, Re et al. 2008).

GABARAP has been suggested to participate in membrane targeting and/or degradation processes. This hypothesis has been supported by the finding that GABARAP interacts with the N-ethylmaleimide-sensitive factor (NSF), a chaperone that activates SNARE proteins in membrane fusion events (Kittler, Rostaing et al. 2001) and also with the clathrin heavy chain (Mohrluder, Hoffmann et al. 2007). Furthermore, GABARAP interacts with gephyrin, a receptor-cytoskeleton linker that interacts with the glycine receptor and polymerized tubulin (Kneussel, Haverkamp et al. 2000).

Originally, a role for GABARAP in the clustering of $GABA_A$-receptors in postsynaptic membranes was proposed (Chen, Wang et al. 2000). Supporting this hypothesis is the finding that overexpression of GABARAP increased the cell-surface number of $GABA_A$-receptors in cultured hippocampal neurons (Leil, Chen et al. 2004) and *Xenopus laevis* oocytes (Chen, Chang et al. 2007). However, the synaptic localization of $GABA_A$-receptors is not affected in $GABARAP^{-/-}$ mice. A possible explanation for this finding could be the functional redundancy of GABARAP with the close related family members GABARAP-L1 and GABARAP-L2 (O'Sullivan, Kneussel et al. 2005).

Interestingly, the core-domain of GABARAP contains an ubiquitin-like fold (Bavro, Sola et al. 2002). It has been shown that GABARAP indeed undergoes a post-translational modification that resembles ubiquitylation. Thus, GABARAP is cleaved at G116, activated by E1- and E2-like enzymes and

finally conjugated to other molecules, most likely phospholipids (Tanida, Komatsu et al. 2003; Sou, Tanida et al. 2006). Insertion of lipopeptides into the membrane could also have an influence the membrane expression of proteins. In this regard, it has been proposed that NaPi-IIa activity and membrane abundance depends on its interactions with lipid microdomains (Breusegem, Halaihel et al. 2005).

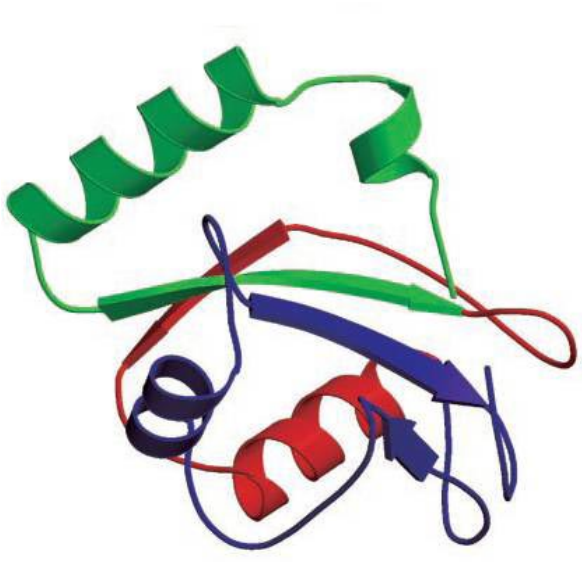

Figure 10: Cartoon diagram of the GABARAP three-dimensional backbone structure.

Amino acids 1–35 are in *green,* amino acids 35–68 are in *red,* and amino acids 68–117 are in *blue*.
The constructs used later in the GST-pull down experiments are amino acids 35–117 (colored in *red* and *blue*) and amino acids 1–68 (colored in *green* and *red*).
(modified from Knight et al., Journal of Biological Chemistry Vol.277, 2002)

4. Aim of the work

The Na-dependend Pi cotransporter NaPi-IIa is expressed in the brush border membrane of renal proximal tubules. Its function is to reabsorb Pi from the primary urine. The apical expression of NaPi-IIa is regulated by hormones and other factors such as the availability of Pi. Apical expression and regulation of NaPi-IIa is controlled by a network of interacting proteins. To identify novel interacting partners a membrane yeast-two-hybrid screening was performed using the functional NaPi-IIa cotransporter as bait. The C-terminal TRL-motif of NaPi-IIa was deleted in order to avoid the numerous interactions with PDZ-proteins that have been shown and studied earlier.

This approach led to the identification of GABARAP as a novel, putative interacting partner of NaPi-IIa. The first aim of my studies was to confirm the expression of GABARAP in renal proximal tubules and to verify the interaction between both partners *in vitro*.

The generation of GABARAP$^{-/-}$ mice has made it possible to study the physiological role of the interaction between GABARAP and NaPi-IIa *in vivo*. Therefore, in the second part of my work, my aim was to investigate the effect of the absence of GABARAP on the steady state expression of NaPi-IIa, its hormonal regulation as well as chronic and rapid adaptation to different Pi diets.

5. Material and Methods

5.1 Animal Studies

GABARAP$^{-/-}$ mice were derived from a library (Omnibank) of embryonic stem cells in which various genes were inactivated by gene-trap methodology based on insertion of a huge viral vector (Zambrowicz, Friedrich et al. 1998). One of the clones was used to generate a heterozygous GABARAP mouse by blastocyst injection (Lexicon Pharmaceuticals, Texas, USA). GABARAP$^{-/-}$ mice were generated from transgenic 129SvEvBrd embryonic stem cells, injected into C57Bl/6J albino blastocyts and back crossed for 7 generations with the C57Bl/6J line. All experiments were performed with 12-16 weeks old mice.

5.1.1 Genotyping of mice

Genomic DNA was extracted from tail tissue of the mice. Briefly, ~2 mm tail tissue was dissolved in 500 µl lysis buffer containing 100 mM Tris-HCl pH 8.5, 5 mM EDTA, 0.2% SDS, 200 mM NaCl and 0.1 µg/µl proteinase K by over night incubation at 55 ºC. Undigested material was pelleted by centrifugation in a microfuge at full speed for 5 min. Genomic DNA was precipitated by adding 500 µl isopropanol to the supernatant and inversion of the tube for ~20 times. The DNA was pelleted and subsequently washed with 70% EtOH. After washing, the pellet was dried and finally resuspended in 100 µl TE buffer containing 10 mM Tris-HCl pH 8 and 1 mM EDTA.

For genotyping, 1 µl of the genomic DNA was used for each of the two PCRs. The two different sets of primers which were used are indicated below. The PCR was performed using the Taq-Polymerase (Sigma) and 35 cycles. The annealing temperature was either 60 °C (primer pair 1) or 64 °C (primer pair 2). Elongation time was 2 min in both PCR reactions.

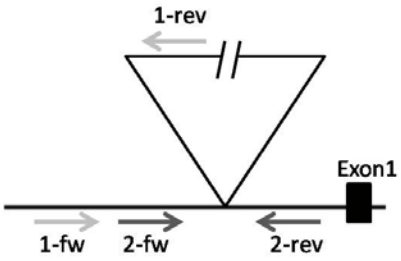

genotype	expected PCR products	
	primer pair 1 1-fw: 5`-ACTGGATGGAGTCCCTGATG-3` 1-rev: 5`-GAGTGATTGACTACCCGTCAGCG-3`	primer pair 2 2-fw: 5`-CCACCTTCAGCGTAGAAAC-3` 2-rev: 5`-GCCTGCTAACATACGCCACT-3`
+/+	-	300 bp
+/-	640 bp	300 bp
-/-	640 bp	-

Figure 11: Schematic model of the genotyping of GABARAP$^{-/-}$ mice.

5.1.2 Animal treatments

For metabolic studies, mice were housed separately in metabolic cages with free access to food and water. Urine was collected under mineral oil. Blood was withdrawn from the vena cava of anesthetized mice. Urinary and plasma ion composition was analyzed by Ion Chromatography (Metrohm 820 Professional IC). Creatinine and Pi concentrations were determined according to the Jaffe (Wako Chemicals) and Fiske Subarov methods (Sigma Diagnostics) respectively. Urinary concentration of cAMP was determined using a cAMP [^{3}H] assay system (Amersham).

For PTH-injections mice were injected i.p. with 0.5 µg/g body weight of 1-34 PTH (Sigma) or with 0.9% NaCl as control. Kidneys were harvested 45 minutes after injection and rapidly frozen until further use.

For dietary adaptation, mice were fed either with a high (1.2%) or a low (0.1%) Pi diet (Kliba, NAFAG) and had free access to water. In order to study the acute effect of dietary Pi, the mice were trained to receive food only for 4 hours daily to time food intake.

All animal experiments were performed according to Swiss Animal Welfare laws, with approval of the local veterinary authority (Kantonales Veterinäramt Zürich).

5.2 Plasmids

To obtain GST-fusion constructs, PCR products encoding either full length or amino acids 1-68 and 36-117 of GABARAP were subcloned into the

BamHI/SalI site of pGEX-TK-Ras (Zhao, Lim et al. 2001). To generate myc-fused GABARAP, nucleotide sequences encoding the myc epitope (EQKLISEEDL) immediately preceded by a Kozak consensus sequence were first introduced into the pcDNA3.1 plasmid (Invitrogen) by bi-directional PCR with overhanging primers followed by subsequent phosphorylation and ligation. Then, full-length GABARAP was subcloned into the myc-pcDNA3.1 plasmid using XhoI/KpnI restriction sites. Mouse NaPi-IIa was subcloned into the mammalian expression vector pHA-MEX (Dualsystems Biotech) using XhoI/EcoRI restriction sites. Generation of NaPi-IIa ΔL571 has been described elsewhere (Karim-Jimenez, Hernando et al. 2001).

5.3 Expression of GST-fusion proteins in E.coli

XL-1 blue competent cells were transformed with the respective plasmid by heat-shock and plated on a LB-agar plate (10 g/l Bacto tryptone, 5 g/l yeast extract, 10 g/l NaCl and 15 g/l agar) containing 100 µg/ml ampicillin. An overnight culture was set up in 50 ml LB medium supplemented with 2% D-glucose and 100 µg/ml ampicillin. The next day, 20 ml of this culture were diluted in 500 ml LB-medium containing D-glucose and ampicillin. The culture was further incubated at 37 ºC to an OD_{600} of 0.6 to 0.8. Then, isopropyl-1-thio-β-D-galactoside (IPTG) was added to a final concentration of 1 mM. The incubation of the culture was continued for 14 hrs at 25 ºC. The bacteria were pelleted by centrifugation at 5000 g for 10 min at 4 ºC. The supernatant was discarded and the pellet was resuspended in 8 ml lysis buffer (Tris-HCl pH 8, 120 mM NaCl, 0.5% Igepal CA-630, 5 mM DTT, 1 mM EDTA, 2 mg/ml lysozyme, 1 µg/ml leupeptin, 1 mM PMSF and Roche protease inhibitor cocktail). After 15 min on ice, the lysis of the bacteria was completed by sonication for 30 sec (pulsed, stage 3, 30% cycle) twice. The solubilized bacteria were centrifuged at full speed in a microfuge at 4 ºC for 15 min. The supernatants were shock frozen in liquid nitrogen and stored at -80 ºC until further usage.

In order to estimate the amount of GST-fusion proteins in the bacteria lysates, glutathione agarose beads (Sigma) were equilibrated in buffer I

containing 50 mM Tris-HCl pH 8, 120 mM NaCl, 0.5% Igepal CA-630 and 5 mM DTT. After a short centrifugation, 250 µl of the same buffer and 50 µl E.coli extract were added to the beads. The mixture was then incubated for 60 min at 4 °C on a rotary shaker. Next, the beads were washed twice with 500 µl buffer I containing 0.075% SDS. Proteins were eluted by incubation in 50 µl loading buffer at 95 °C for 5 min. Samples (25 µl) were subsequently analyzed on a SDS-PAGE with BSA standards of known protein concentration. After completing electrophoresis, the gel was stained with Coomassie blue and the protein concentration of the GST-proteins was estimated.

5.4 Preparation of brush border membrane vesicles (BBMV)

BBMV were prepared using the Mg^{2+}-precipitation technique (Biber, Stieger et al. 2007). Kidneys were cut into small pieces in a glass petri dish on ice and transferred into 800 µl ice-cold homogenization buffer containing 300 mM mannitol, 5 mM EGTA and 12 mM Tris-HCl, pH 7.1. Then, the kidneys were homogenized for 2 min on ice using a polytron (Kinematica). Upon addition of 1120 µl water and 22 µl of 1M $MgCl_2$ (12 mM final) samples were precipitated on ice for at least 15 min.

Scraped mucosa of the ileum of the small intestine was mixed with 200 µl ice-cold homogenization buffer and 1000 µl of water and then homogenized using an Omnimixer at speed 5 for 1 min. Samples were transferred into an eppendorf tube and 11 µl of 1M $MgCl_2$ (10 mM final) was added. BBM were precipitated on ice for at least 30 min.

Then, the samples (from kidney/intestine) were centrifuged in a Sorvall centrifuge (rotor SS34) for 15 min at 4500 rpm. Small aliquots of supernatants, representing total homogenates, were immediately frozen, whereas the rest was further centrifuged at 18500 rpm for 30 min. The pellet was resuspended in 1 ml of membrane buffer (300 mM mannitol, 20 mM Hepes-Tris, pH 7.4) and centrifuged again at 18500 rpm for 30 min. After removing the supernatant, the pellet containing the BBMV was resuspended in 150 µl of membrane buffer. Finally, protein concentration was measured using a BioRad protein determination kit (Lowry method).

5.5 Glutathione S-Transferase Pull-Downs

GST pull-downs were performed with isolated BBM or HEK293 cell lysates. In order to couple GST-protein to Glutathione agarose-beads (Sigma), 40 µl beads were equilibrated in 1 ml buffer I (see 5.4). After a short centrifugation step (~10 sec in a microfuge) the supernatant was sucked off the beads and 250 µl buffer I was added. E.coli extract containing 50 µg GST-fusion protein (see 5.4) was added to the beads and the mixture was incubated at 4 ºC for at least 1 hr on a rotary shaker. Next, the beads were washed three times either with buffer I and once either with DB-buffer (20 mM Tris-HCl pH 8, 100 mM NaCl, 5 mM EDTA, 10% sucrose, Roche protease inhibitor cocktail) when BBMV were used or with cell lysis buffer (20 mM Tris-HCl pH 8, 100 mM NaCl, 5 mM EDTA, 10% sucrose, 0.75% Triton X-100, 0.75% Na-deoxycholate, Roche protease inhibitor cocktail) for pull-downs from transfected cells.

For GST-pull downs from BBMV, the membranes were first solubilized as follows: 50 µg BBMV were diluted in SB-A buffer (20 mM Tris-HCl pH 8, 5 mM EDTA, 10% glycerol, 1 mM PMSF, 5 µg/ml leupeptin, 5 µg/ml pepstatin A) in a final volume of 50 µl. Then, 50 µl SB-A containing 1% Na-deoxycholate was added and mixed gently by pipetting. After incubation for 1 hr at room temperature, undissolved membranes were removed by centrifugation at full speed in a microfuge at 4 ºC for 30 min. The supernatant was added to the GST-coupled beads which were resuspended in 1.2 ml DB-buffer after the washings.

For GST-pull downs from transfected HEK293 cells, cultures (10 cm dish) were lysed in 1.2 ml cell lysis buffer and incubated on ice for 15 min. Then, lysates were passed 10 times through a syringe with a 25G needle. Cellular debris was removed by centrifugation at full speed in a microfuge for 30 min at 4 ºC. 35 µl Glutathione agarose beads were equilibrated in cell lysis buffer and added to the supernatants. After preclearing for 1 hr at 4 ºC on a rotary shaker, beads were pelleted by short centrifugation and the cell lysates were added to the GST-coupled beads.

GST-coupled beads were incubated on a rotary shaker over night at 4 °C with solubilized BBM or cell lysate. Then, samples were centrifuged at 13000 g for 1 min. The pelleted beads were washed 5-6 times with TBS containing 0.1% (v/v) Nonidet P-40 and 0.1% (v/v) Tween 20. Proteins were eluted by incubation

in 50 µl loading buffer at 95 °C for 5 min. Samples (25 µl) were subsequently analyzed by Immunoblot.

5.6 Immunoblots

Kidney homogenates or renal BBM were prepared as described before (see 5.5). For Immunoblot analysis, samples obtained from GST-pull downs and co-immunoprecipitation as well as kidney homogenate (40 µg) and renal/intestinal BBM (15 µg) were separated on 9% SDS/PAGE gels, transferred to PVDF membranes and then incubated over night at 4 °C with antibodies against NaPi-IIa (Custer, Lotscher et al. 1994), NaPi-IIc (Nowik, Picard et al. 2008), PDZK1 (Gisler, Stagljar et al. 2001), NHERF-1 (Abcam), GABARAP (Green, O'Hare et al. 2002) and β-actin (Sigma). After incubation with HRP-linked secondary antibodies (GE Healthcare), immunoreactive signals were detected by chemiluminescence (ECL, Amersham Pharmacia Biotech) using the DIANA III-chemiluminescence detection system (Raytest). The densitometry of all images was analyzed using appropriate software (Advanced Image Data Analyser AIDA, Raytest) to calculate, for each given experiment, the ratio between the protein of interest to β-actin.

5.7 Cell culture

HEK293 cells were plated in 10 cm dishes and cultured in DMEM supplemented with 10% FCS, 5 mM L-Glutamine, 100 U/ml penicillin and 100 U/ml Streptomycin in 5% CO_2 at 37 °C. Subconfluent cultures were transfected with 6 µg plasmid using Lipofectamine 2000 (Invitrogen) according to the manufacturer`s instructions. All experiments were performed 48 hrs after transfection.

5.8 Co-Immunoprecipitation

Two days after transfection cells were lysed in 1 ml IP-buffer containing 50 mM Tris pH 7.4, 72 mM NaCl, 0.75% Triton X-100, 0.75% Na-deoxycholate, 1 mM PMSF, 5 µg/µl Leupeptin, 5 µg/µl Pepstatin A. After pre-clearing with 40 µl Protein G Plus/ Protein A agarose beads (Calbiochem) the anti-myc antibody (Invitrogen) was added in a dilution of 1:250. After incubation at 4 ºC on a rotary shaker over night, 50 µl Protein A/G beads were added to the lysates and further incubated at 4 ºC on a rotary shaker for 60 min. Protein G Plus/ Protein A agarose beads were pelleted by short centrifugation steps (microfuge) and washed 4 times with IP-buffer containing detergents and once with IP-buffer without detergents. Proteins were eluted by incubation in loading buffer at 95 °C for 5 min. Samples were subsequently analyzed by Immunoblot.

5.9 Uptake in isolated BBMV

The Na^+-dependent transport rate of $^{32}P_i$ into renal BBMV was determined in the presence of 0.1 mM potassium phosphate as described previously (Biber, Stieger et al. 1981). Briefly, 10 µl BBMV were added to 40 µl solution A for sodium-dependent transport (100 mM Mannitol, 20 mM HEPES-Tris pH 7.4, 125 mM NaCl, 0.125 mM Pi pH7.4) or solution B to measure sodium-independent transport (100 mM Mannitol, 20 mM HEPES-Tris pH 7.4, 125 mM KCl, 0.125 mM Pi pH 7.4). 40 µl of each solution (A or B) contained 1-2 µCi ^{32}P (as orthophosphoric acid). Transport of ^{32}P was determined at 25 ºC. To terminate the reaction after the desired time point (30 sec, 1 min, 120 min), 20 µl of solution A or solution B containing the BBMV were pipetted into 1 ml ice-cold Stop-solution consisting of 100 mM Mannitol, 150 mM NaCl, 5 mM Tris-HCl pH 7.4, 5 mM Pi pH 7.4. After vortexing, the sample was spotted onto a membrane (Sartorius) placed on a vacuum pump system. Then the membrane was washed with ~6 ml Stop-solution and put into a scintillation vial for counting.

Similar protocols were used to measure uptake of radioactively labeled L-Glutamine and D-Glucose.

5.10 RNA Isolation and Real-Time PCR

Total RNA was extracted from kidneys homogenized in RLT buffer using the RNeasy Mini Kit (Qiagen). Similarly, RNA from dissected nephron segments was extracted using the RNeasy Micro Kit (Qiagen) according to manufacturer`s instructions. Either 300 ng of RNA from total kidney or 80 ng of RNA from nephron segments were used as template for reverse transcription using TaqMan Reverse Transcription Kit (Applied Biosystems). Real-Time PCR was performed on the ABI PRISM 7700 Sequence Detection System, using commercial primers and probes for NHERF1 and GABARAP (Taqman Gene Expression Assays) as well as primers and probes for NaPi-IIa and NaPi-IIc (Madjdpour, Bacic et al. 2004) and β-ENaC (Fakitsas, Adam et al. 2007). Amplification was carried out using the TaqMan Universal PCR Master Mix (PCR machine and reagents from Applied Biosystems). The expression of the gene of interest was calculated in relation to hypoxanthine guanine phosphoribosyl transferase (HPRT). Relative expression ratios were calculated as $R = 2^{[Ct(HPRT)-Ct(test\ gene)]}$, where Ct represents the cycle number at the threshold 0.2.

5.11 Immunostainings

Mouse kidneys were perfusion-fixed through the right ventricle with a fixative solution containing freshly made 3% paraformaldehyde, 3 mM $MgCl_2$, 4.5 mM picric acid in a 6:4 mixture of 0.1 M cacodylate buffer (pH 7.4; adjusted to 300 mOsm with sucrose) and 10% hydroxyethyl starch (HAES). Subsequent immunohistochemistry was performed as described previously (Dawson, Gandhi et al. 1989). Briefly, cryosections (6 µm) were taken and pretreated with 0.1% SDS (NaPi-IIa and NaPi-IIc) or 0.5% SDS (NHERF1/2 and 4F2) for 5 min followed by three washes in PBS for 5 min each. After blocking with 2% BSA, 0.02% Na-azide in PBS, sections were incubated at 4°C overnight with antibodies against NaPi-IIa 1:600 (Custer, Lotscher et al. 1994), NaPi-IIc 1:400 (Nowik, Picard et al. 2008), NHERF1/2 1:300 (Capuano, Bacic et al. 2005) and CD98 (4F2) 1:200 (Santa Cruz) in blocking solution. After three washings in PBS for 5 min each, binding sites of the primary antibodies were detected using

Alexa 488-conjugated anti-rabbit/Alexa 568-conjugated anti-goat antibodies (Invitrogen). F-actin was visualized using Texas-Red-coupled phalloidin which was added in a dilution of 1:100 (Invitrogen). The sections were washed again three times in PBS for 5 min each washing and then mounted with mounting medium (DACO). Sections were analyzed with an inverted epi-fluorescence microscope (Nikon Eclipse TE300).

5.12 Determination of mineral concentrations in bone ashes

The concentration of Pi and Ca^{2+} in lumbar vertebrae (L3 and L4) and femurs was determined as follows. Bones were extracted from the mice and frozen at -20 °C until further use. Then, the bones were first dried for 96 hrs at 105 °C and afterwards put in a muffle furnace at 600 °C for 96 hrs to obtain bone ash. The ashes were resuspended in 8% HCl and then filtered. The minerals were determined by colorimetry with an autoanalyzer (COBAS MIRA, Roche) using commercial kits. Analyses of Pi and Ca^{2+} were based on the the phosphomolybdate and the methylthymol blue method, respectively (Liesegang, Loch et al. 2005).

6. Results

6.1 Renal Expression of GABARAP and interaction with NaPi-IIa

Using a classical yeast-two hybrid (YTH) screen, we previously identified several proteins that interact with the C-terminal intracellular tail of NaPi-IIa (Gisler, Stagljar et al. 2001). Most of these interactions were PDZ-based and depended on the last 3 residues of NaPi-IIa (TRL). Classical YTH analysis requires soluble baits to screen for protein-protein interactions. In comparison, the advantage of the split-ubiquitin membrane YTH system (MYTH) is that full-length integral membrane proteins can be used as baits (Stagljar, Korostensky et al. 1998; Gisler, Kittanakom et al. 2008). We used the MYTH 2.0 system to screen a mouse kidney library targeting the identification of interactions independent on the C-terminal PDZ-binding domain of NaPi-IIa. To this end, we used the TRL-truncated (instead of full-length) cotransporter as bait. Three interacting clones were identified as GABARAP. Two of these clones contained the full length open reading frame (ORF), whereas the third cDNA was a partial fragment that lacked the first 34 nucleotides of the ORF. The GABARAP protein consists of 117 amino acids and shares similarity with the light chain-3 of microtubule-associated proteins 1A and 1B (Wang, Bedford et al. 1999).

6.1.1 Expression of GABARAP in the kidney

Expression of GABARAP was first verified using RT-PCR from total kidney RNA with primers spanning intron-exon boundaries (data not shown). To further address the distribution of GABARAP mRNA within the kidney, Real-Time PCR was performed on dissected murine nephron segments. GABARAP mRNA was found to be uniformly expressed in all tested nephron segments (Fig. 12A).

To rule out cross-contaminations with mRNA from different nephron segments, I analyzed the profile of known marker genes differentially expressed along the nephron. As marker for proximal tubules, NaPi-IIa expression was determined in the nephron segments. NaPi-IIa mRNA was highly abundant in

proximal convoluted tubules (S1+2) and expressed to a lesser extend in proximal straight segments (S3) whereas expression in more distal segments was hardly detectable (Fig. 12B). As a marker for distal nephron segments, I determined the expression of β-ENaC mRNA which was highly abundant in our preparation of CCD and absent in proximal segments (Fig. 12B).

In order to confirm GABARAP protein expression, an Immunoblot using an antibody raised against human GABARAP (Green, O'Hare et al. 2002) was performed on murine renal BBM preparations (Fig. 12C). In addition to the band at the expected molecular weight of 17 kDa (Wang, Bedford et al. 1999), I observed a second product of faster mobility which most likely represents a lipidated form of GABARAP (Tanida, Ueno et al. 2004). None of these bands were detected in BBM preparations of GABARAP$^{-/-}$ mice, confirming the specificity of the signal.

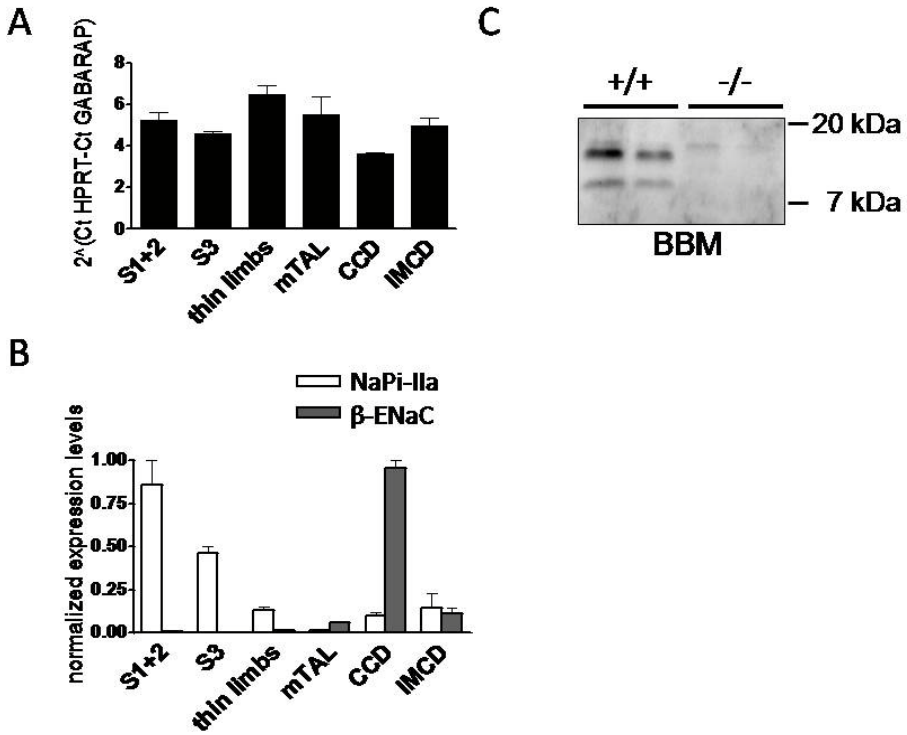

Figure 12: Renal expression of GABARAP mRNA and protein.

Quantification of **(A)** GABARAP and **(B)** NaPi-IIa and β-ENaC mRNAs in dissected nephron segments. The abundance of GABARAP, NaPi-IIa and β-ENaC mRNA was measured by Real-Time PCR. Values were normalized to Hypoxanthine-guanine phosphoribosyltransferase (HPRT) (n=2). For NaPi-IIa and β-ENaC, the highest value was set as 1 and used to normalize the other values. **(C)** Immunoblot analysis to detect the presence of GABARAP in renal BBM. BBM isolated from GABARAP$^{-/-}$ mice were used to show specificity of the antibody.

6.1.2 Interaction between NaPi-IIa and GABARAP

The interaction of GABARAP and NaPi-IIa was verified by pull-downs of NaPi-IIa from BBM using GST-GABARAP and by co-immunoprecipitation from transfected HEK293 cells. In the pull-down assay, a band at the expected molecular weight for NaPi-IIa was detected using GST-GABARAP but not with GST alone (Fig. 13A). In addition, I tested two overlapping halves of GABARAP (aa 1-68 and aa 37-117, respectively) for their ability to interact with NaPi-IIa. As shown in figure 13A, both GST-fusion proteins were capable of pulling down NaPi-IIa from BBM. In the lower panel, a Ponceau staining of the membrane is shown to demonstrate the use of similar amounts of the GST-fusion proteins in the different pull downs.

The specific interaction between NaPi-IIa and GABARAP was further confirmed by co-immunoprecipitation of myc-tagged GABARAP and NaPi-IIa from transfected HEK293 cells (Fig. 13B). Cells were transfected either with NaPi-IIa alone or cotransfected with NaPi-IIa and myc-GABARAP. Then, an antibody against the myc-epitope was used to immunoprecipitate myc-GABARAP. A band with the expected molecular weight for NaPi-IIa was seen only in the immunoprecipitation from cotransfected cells in the presence of myc-antibody (Fig. 13B top panel) but not in negative controls lacking either myc-GABARAP or the anti myc-antibody. As expected, myc-GABARAP was not immunoprecipitated in both negative controls as demonstrated by immunoblots using an anti-myc antibody (Fig. 13B middle panel). Immunoblots on total cell lysates verified the expression of NaPi-IIa and myc-GABARAP in these experiments (Fig. 13B lower panel).

A recent report proposes a consensus sequence for GABARAP-binding sites build around a highly conserved tryptophan residue (Thielmann, Mohrluder et al. 2008). The C-terminal intracellular tail of NaPi-IIa contains a sequence that would fit to this motif. In order to study whether this C-terminal sequence can mediate the interaction with GABARAP, pull downs were performed with lysates from HEK293 cells transfected either with the full length or a C-terminal truncated cotransporter (Δ571). As shown in the top panel of figure 13C, GST alone did not pull down the full length NaPi-IIa whereas both the full length and the truncated NaPi-IIa were pulled down by GST-GABARAP. The Ponceau

staining of the membrane is shown to demonstrate equal loading of the beads with GST-fusion proteins (Fig. 13C, middle panel). Overexpression of NaPi-IIa and NaPi-IIa Δ571 is demonstrated by Immunoblot analysis on total cell lysates (Fig. 13C, lower panel).

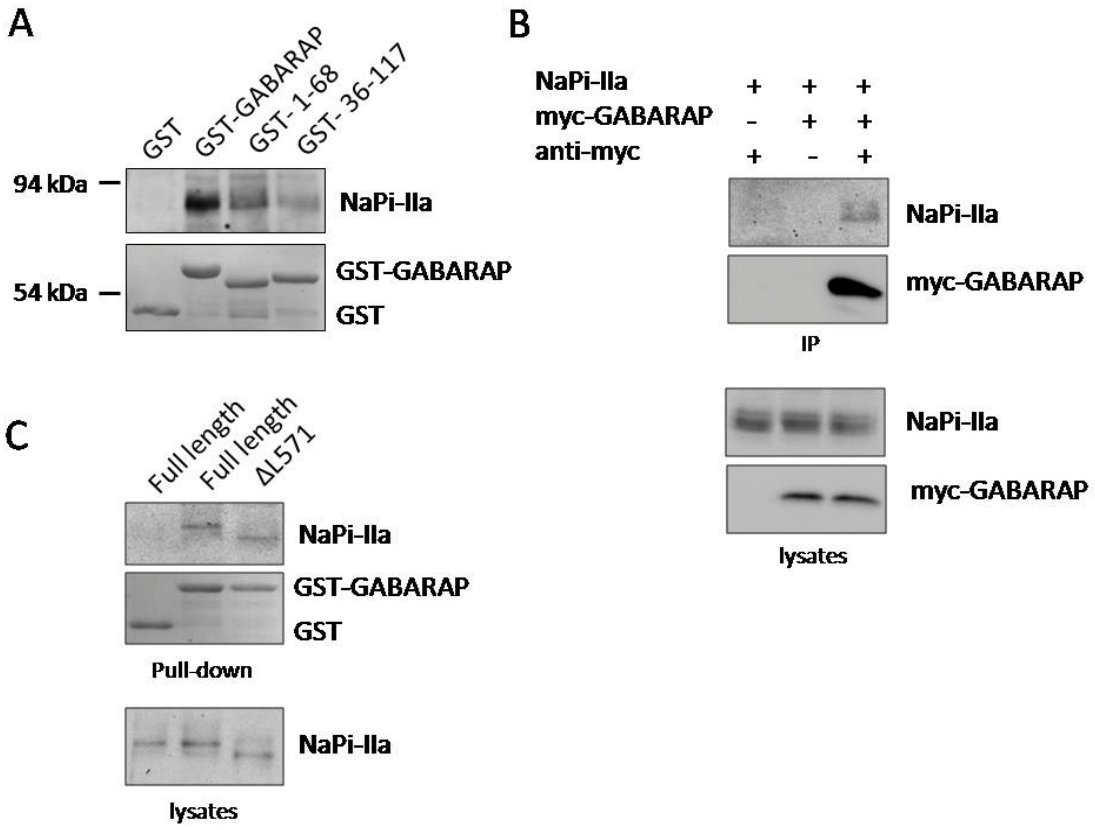

Figure 13: Interaction between NaPi-IIa and GABARAP.

(A) GST-Pull down analysis to show interaction between GABARAP and NaPi-IIa. Full length and overlapping halves of GABARAP were used to pull down NaPi-IIa from BBM. The top panel shows an Immunoblot probed with an anti-NaPi-IIa antibody. The lower panel shows the Ponceau staining of the PVDF-membrane (as grayscale figure) to demonstrate that similar amounts of GST and its fusion proteins were used in the different pull downs. **(B)** Co-immunoprecipitation of NaPi-IIa with myc-GABARAP from cotransfected HEK293 cells. Immunoblots of the immunoprecipitated material (top panels) and HEK293 cell lysates (lower panels) were probed with anti-NaPi-IIa (upper blot) or anti-myc (lower blot) antibodies. **(C)** GST-Pull downs on lysates from HEK293 cells transfected with full length or truncated NaPi-IIa. The top panel shows an Immunoblot of the pulled down material probed with the NaPi-IIa antibody. As negative control, full length NaPi-IIa was incubated with GST (first lane). The middle panel shows the Ponceau staining of the PVDF-membrane (as grayscale figure). The lowest panel shows an Immunoblot on HEK293 cell lysates probed with the NaPi-IIa antibody.

In a further attempt to identify the molecular determinant for the interaction within NaPi-IIa, I fused several discrete intracellular domains of NaPi-IIa to GST in order to pull down GABARAP from transfected HEK293 cells. However, under similar conditions to the ones used in the pull-down experiments described above, I was unable to detect interaction between both partners (data not shown). The failure of these discrete domains of NaPi-IIa to associate with GABARAP could be due either to the need of more than one single intracellular loop for the association or to the requirement of more physiological conditions.

6.2 Analysis of GABARAP$^{-/-}$ mice under normal conditions

6.2.1 Metabolic cage studies with GABARAP$^{+/+}$ and GABARAP$^{-/-}$ mice

In metabolic cage studies, I found that GABARAP$^{-/-}$ mice were slightly though significantly heavier than GABARAP$^{+/+}$ despite the fact that both groups consume similar amounts of food (Table 1). In addition, GABARAP$^{-/-}$ animals drank less water which translated in a reduced urinary output. The reduced urinary excretion tightly correlates with the increased osmolarity and creatinine concentration in the urine from GABARAP$^{-/-}$ animals. Urinary pH as well as urinary cAMP levels were similar in both groups.

Interestingly, the urinary excretion of Pi (as a ratio to creatinine) was significantly reduced in GABARAP$^{-/-}$ as compared to GABARAP$^{+/+}$ mice, whereas excretion of all other tested ions (Cl^-, Na^+, K^+, Mg^{2+} and Ca^{2+}) was similar in both groups when normalized to urinary creatinine (Table 1).

Despite the reduced urinary Pi excretion in GABARAP$^{-/-}$ mice, the concentration of Pi in serum did not differ between both groups (Table 1). The Ca^{2+} concentration in blood was also similar in both groups of animals whereas the circulating levels of Cl^-, Na^+ and K^+ were all increased in GABARAP$^{-/-}$ as compared to GABARAP$^{+/+}$ mice.

	GABARAP$^{+/+}$	GABARAP$^{-/-}$
Metabolic cages		
Body weight (g)	28.48 ± 0.56	30.53 ± 0.34 **
Food intake (mg / g body weight)	0.137 ± 0.005	0.148 ± 0.004
Water intake (ml / g body weight)	0.203 ± 0.010	0.170 ± 0.009 *
Stool (g / g body weight)	0.052 ± 0.004	0.052 ± 0.003
Urine (ml / g body weight)	0.059 ± 0.006	0.041 ± 0.002 **
Urine chemistry		
pH	6.10 ± 0.04	6.15 ± 0.08
Osmolality (mosm/kg H_2O)	2494 ± 164	3634 ± 124 ***
Creatinine (mg/dl)	59.28 ± 4.28	94.96 ± 5.93 ***
cAMP (pmol) / creatinine (mg/dl)	25.14 ± 0.91	23.68 ± 0.68
Na^+ (mM) / creatinine (mg/dl)	1.95 ± 0.11	1.80 ± 0.10
K^+ (mM) / creatinine (mg/dl)	7.15 ± 0.23	7.02 ± 0.38
Ca^{2+} (mM) / creatinine (mg/dl)	0.037 ± 0.009	0.032 ± 0.003
Mg^{2+} (mM) / creatinine (mg/dl)	0.62 ± 0.02	0.56 ± 0.03
P_i (mM) / creatinine (mg/dl)	1.79 ± 0.07	1.24 ± 0.09 ***
Cl^- (mM) / creatinine (mg/dl)	5.13 ± 0.38	4.32 ± 0.24
Blood chemistry		
Na^+ (mM)	143.3 ± 0.33	146 ± 0.86 **
K^+ (mM)	3.84 ± 0.09	4.39 ± 0.18 *
Ca^{2+} (mM)	1.28 ± 0.01	1.27 ± 0.01
P_i (mM)	2.54 ± 0.06	2.66 ± 0.14
Cl^- (mM)	110.5 ± 0.45	112.1 ± 0.64 *

Table 1: Metabolic cage studies and urine/blood analysis of GABARAP$^{-/-}$ and GABARAP$^{+/+}$ mice.

Values are means ± SEM with either n=15 mice per group (for metabolic cage data and urine analysis) or n=10 mice per group (for blood analysis). (*p ≤ 0.05, **p ≤ 0.01, ***p ≤ 0.0001, unpaired student t-test)

6.2.2 NaPi-IIa and NaPi-IIc expression in GABARAP$^{+/+}$ and GABARAP$^{-/-}$ mice

NaPi-IIa is the major regulator of renal Pi handling and the absence of the NaPi-IIa interacting partner GABARAP results in a reduced urinary excretion of Pi (Table 1). Therefore, I next studied whether the interaction with GABARAP has an influence on NaPi-IIa expression. For that purpose I performed Immunoblot analysis on BBM isolated from GABARAP$^{+/+}$ and GABARAP$^{-/-}$ mice. In these experiments, β-actin was used as loading control and to normalize the expression levels. NaPi-IIa abundance was increased approximately two-fold in renal BBM of GABARAP$^{-/-}$ as compared to GABARAP$^{+/+}$ mice (Fig. 14A). The expression of a second Na-dependent Pi cotransporter, NaPi-IIc, was similar in both groups (Fig. 14B).

As a next step I analyzed whether the difference in NaPi-IIa protein abundance involves changes on the transcriptional level. Therefore, I quantified the amount of NaPi-IIa mRNA in kidneys from GABARAP$^{+/+}$ and GABARAP$^{-/-}$ mice by Real-Time PCR. As shown in figure 14C both groups of animals had similar levels of NaPi-IIa mRNA, suggesting that upregulation of the cotransporter in GABARAP$^{-/-}$ mice is independent on transcriptional changes. In addition, NaPi-IIc mRNA expression was compared between GABARAP$^{+/+}$ and GABARAP$^{-/-}$ mice and its levels were similar in both groups.

Immunohistochemistry was performed to determine whether the loss of GABARAP alters the segmental and/or subcellular distribution of NaPi-IIa. In addition the pattern of expression of NaPi-IIc was also analyzed. It has been shown earlier that NaPi-IIa expression is highest in proximal convoluted tubules (S1, S2) and gradually decreases towards the end of the proximal straight tubule (S3) with a decreasing gradient from juxtamedullary to superficial nephrons (Custer, Lotscher et al. 1994). In adults, NaPi-IIc expression is found preferentially in S1 segments of proximal convoluted tubules of juxtamedullary nephrons (Segawa, Kaneko et al. 2002; Ohkido, Segawa et al. 2003). As shown in figures 15A and B, the segmental distribution and subcellular localization of NaPi-IIa and NaPi-IIc were not altered in kidneys from GABARAP$^{-/-}$ as compared to GABARAP$^{+/+}$ mice.

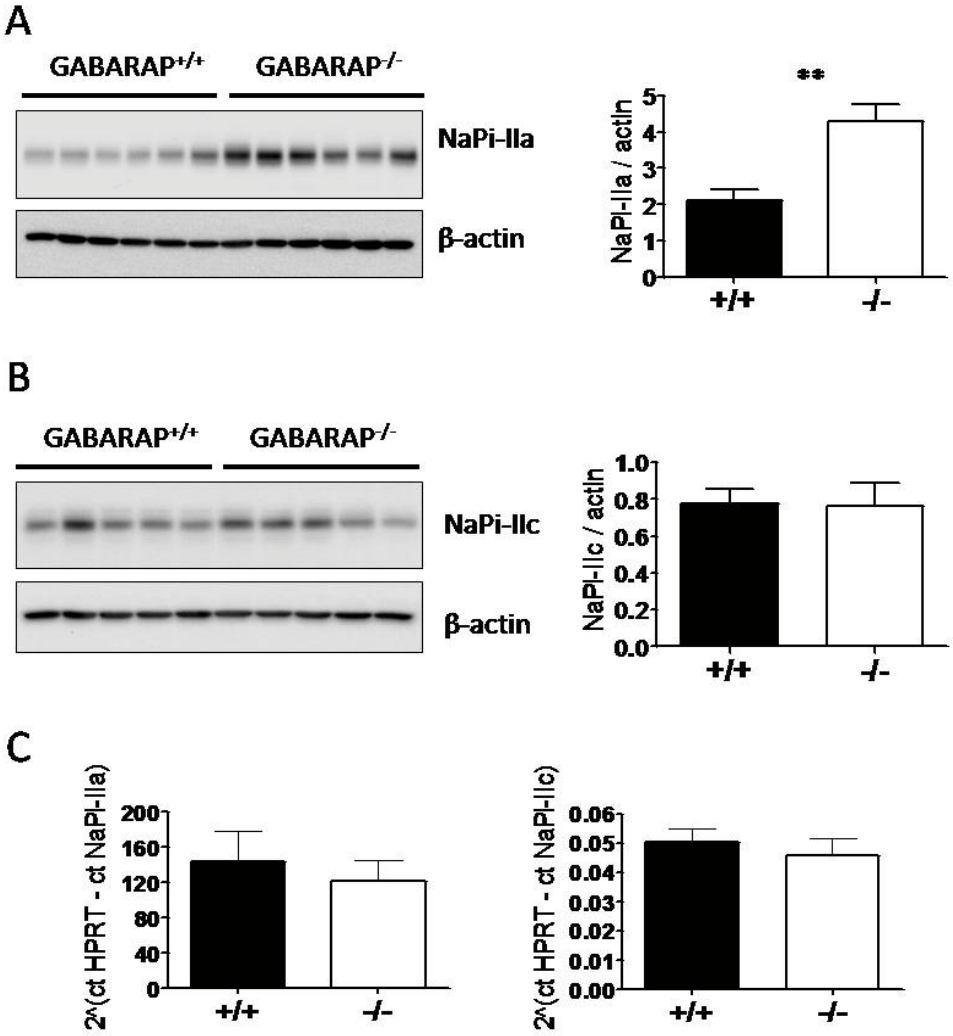

Figure 14: Expression of NaPi-IIa and NaPi-IIc protein and mRNA in GABARAP$^{-/-}$ and GABARAP$^{+/+}$ mice.

Immunoblot on renal BBM isolated from GABARAP$^{+/+}$ and GABARAP$^{-/-}$ mice to analyze the expression of **(A)** NaPi-IIa and **(B)** NaPi-IIc. Expression of both transporters was normalized to the abundance of β-actin for the quantification. **(C)** Real-Time PCR to determine mRNA levels of NaPi-IIa (left) and NaPi-IIc (right) on mRNA extracted from kidney. NaPi-IIa and NaPi-IIc mRNA expression was normalized to HPRT (n=6). Data are means ± SEM. (** $p \leq 0.01$, unpaired student t-test).

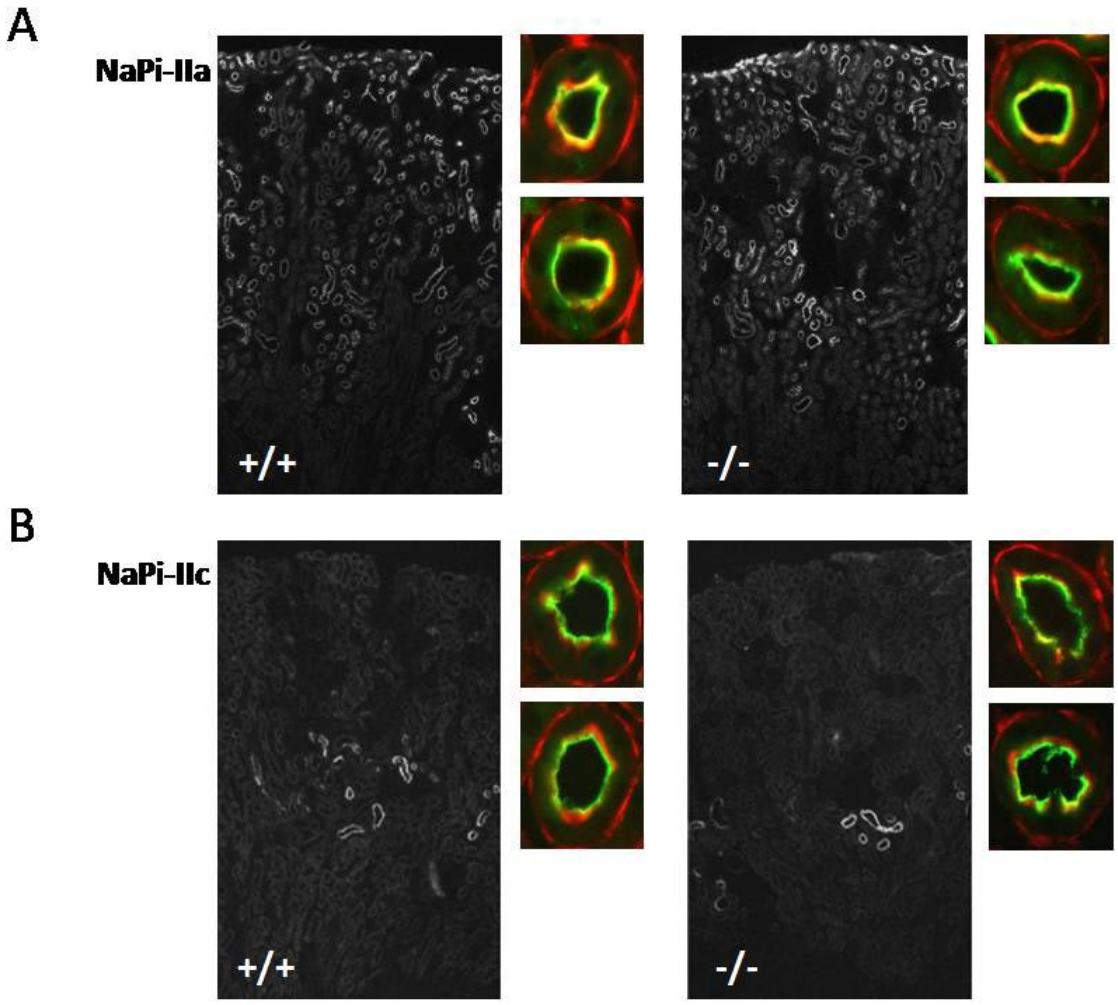

Figure 15: Immunohistochemical analysis of NaPi-IIa and NaPi-IIc in GABARAP$^{+/+}$ and GABARAP$^{-/-}$ mice.

Immunostaining of **(A)** NaPi-IIa and **(B)** NaPi-IIc on kidney cryosections obtained from GABARAP$^{+/+}$ (left) and GABARAP$^{-/-}$ mice (right). Renal cortical overviews are displayed as grayscale figure. The images of single proximal tubules show **(A)** NaPi-IIa and **(B)** NaPi-IIc, both green, co-stained with β-actin (red) as a marker for BBM.

6.2.3 Pi transport activity into BBMV from GABARAP$^{+/+}$ and GABARAP$^{-/-}$ mice

In order to test whether the increased amount of NaPi-IIa in GABARAP$^{-/-}$ mice also translates into an increased Pi transport acitvity, I measured Na^+-dependent uptake of ^{32}Pi into BBMV. As shown in figure 16, Na-dependent uptake of Pi was significantly higher in BBMV prepared from GABARAP$^{-/-}$ as compared to GABARAP$^{+/+}$ mice. As a control, uptake of L-glutamine and D-glucose into the same preparations of BBMV was determined (Fig. 16). The lack of GABARAP specifically upregulates Na^+/P_i-cotransport in BBM since Na^+-dependent uptake of L-Glutamine and D-Glucose were both not altered. The effect observed in the transport studies is smaller than the increase on the expression of NaPi-IIa in GABARAP$^{-/-}$ mice seen in Immunoblots (Fig. 14A). This is likely due to the presence of other Na^+-dependent Pi cotransporters, such as NaPi-IIc, which also contribute to the Na^+/Pi-uptake in renal BBM.

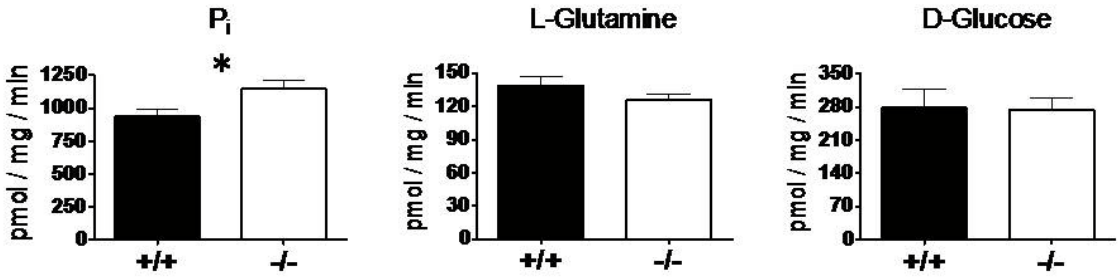

Figure 16: Na^+-dependent uptake into renal BBMV.

Na^+-dependent uptake of Pi (n=10), L-Glutamine (n=4) and D-Glucose (n=5) into BBMV isolated from kidneys of GABARAP$^{-/-}$ and GABARAP$^{+/+}$. Uptakes were analyzed after 1 minute incubation as indicated. Data are means ± SEM. (* $p \leq 0.05$, unpaired student t-test)

6.2.4 Expression of known NaPi-IIa interacting proteins in GABARAP$^{-/-}$ mice

I next analyzed whether the increased expression of NaPi-IIa in the BBM of GABARAP$^{-/-}$ mice is associated with changes in known NaPi-IIa interacting proteins. My interest was focused especially on the well studied members of the NHERF-family, namely NHERF1 and PDZK1. As shown in figure 17A, the abundance of NHERF1 was dramatically increased in kidney homogenates of GABARAP$^{-/-}$ as compared to GABARAP$^{+/+}$ mice. Most likely, the products of different mobility in SDS-gels represent distinctly phosphorylated NHERF1. In contrast to NHERF1, the expression of PDZK1 was similar in both groups based on immunoblot data.

In order to determine whether the upregulation of NHERF1 protein is due to an increased gene expression, I performed RealTime PCR for NHERF1 on total kidney RNA from GABARAP$^{+/+}$ and GABARAP$^{-/-}$ mice. As for NaPi-IIa, upregulation of NHERF1 is independent on changes at the transcriptional level, since NHERF1 mRNA abundance was not altered in GABARAP$^{-/-}$ mice (Fig. 17B).

Surprisingly, no change of NHERF1 signal intensity or subcellular localization could be detected in immunofluorescence stainings of kidney cryosections obtained from GABARAP$^{+/+}$ and GABARAP$^{-/-}$ mice (Fig. 17C). Of note, different antibodies were used for the immunoblots (Fig. 17A) and immunofluorescence (Fig. 17C) experiments. Immunoblots were performed with a commercial antibody that specifically recognizes NHERF1. However, this antibody failed to give a specific signal in immunostainings. Therefore, a different antibody had to be used in the immunofluorescence studies. The failure to detect NHERF1 changes between kidney cryosections from GABARAP$^{-/-}$ and GABARAP$^{+/+}$ mice could be due to crossreaction of this second antibody with the NHERF2 isoform.

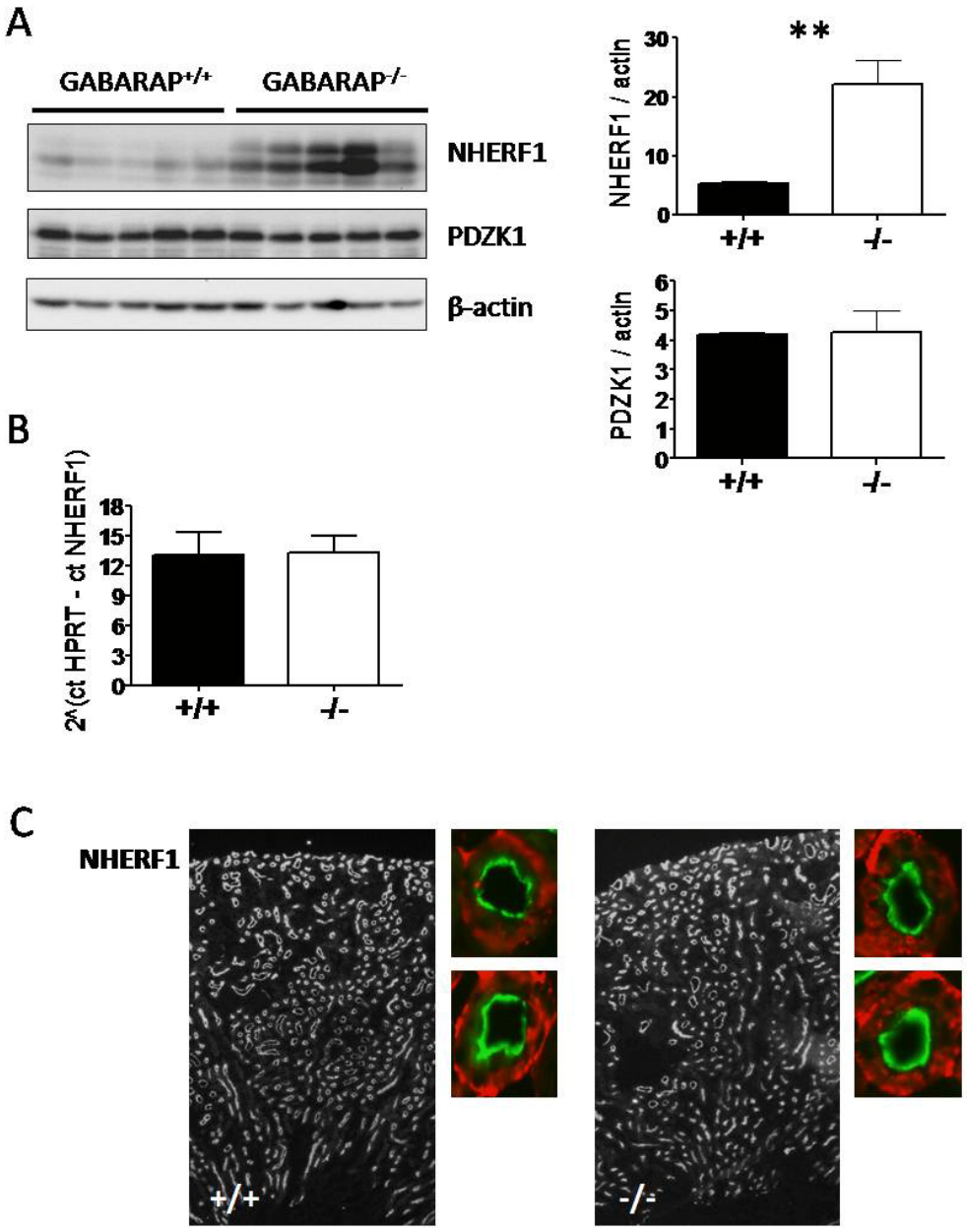

Figure 17: Renal expression of NHERF1 and PDZK1 in GABARAP$^{-/-}$ and GABARAP$^{+/+}$ mice.

(A) Immunoblot analysis of NHERF1 and PDZK1 on homogenates of kidneys extracted from GABARAP$^{+/+}$ and GABARAP$^{-/-}$ mice. For quantification, expression was normalized to β-actin. **(B)** Real-Time PCR to determine NHERF1 mRNA levels normalized to HPRT (n=6). Data are means ± SEM. (** $p \leq 0.01$, unpaired student t-test) **(C)** Immunostaining of NHERF1 on kidney cryosections obtained from GABARAP$^{+/+}$ (left) and GABARAP$^{-/-}$ mice (right). Renal cortical overviews are displayed as grayscale figure. The images of single proximal tubules show NHERF1 (green) and CD98/4F2 (red) as marker for proximal tubules.

6.2.5 Expression of NaPi-IIb in the small intestine

Despite the increased renal Pi reabsorption in GABARAP$^{-/-}$ mice compared to GABARAP$^{+/+}$ animals, serum Pi levels are similar in both groups (Table 1). Therefore, a compensatory mechanism must exist to balance Pi levels in the absence of GABARAP. Up to now, NaPi-IIb is the only NaPi cotransporter with a clear implication in intestinal absorption of Pi, and its expression in mice is known to be higher in the ileum than in other intestinal segments. To address whether a lower Pi absorption in the small intestine could mediate the compensatory effect, I analyzed the expression of NaPi-IIb in BBM prepared from scraped mucosa of the ileum. Again, β-actin was used as loading control and to normalize NaPi-IIb expression levels. The immunoblot data suggest that NaPi-IIb abundance is decreased in the small intestine of GABARAP$^{-/-}$ compared to GABARAP$^{+/+}$ mice (Fig. 18).

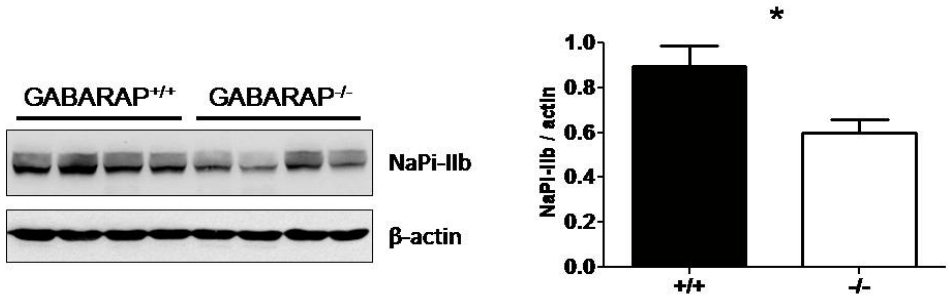

Figure 18: Expression of NaPi-IIb in BBM of the small intestine.

Immunoblot on BBM isolated from the ileum of GABARAP$^{+/+}$ and GABARAP$^{-/-}$ mice to analyze the expression of NaPi-IIb. Expression of NaPi-IIb was normalized to the abundance of β-actin for the quantification.

6.2.6 Pi and Ca^{2+} content in the bones of GABARAP$^{+/+}$ and GABARAP$^{-/-}$ mice

As described before, in addition to the kidney and the intestine, bone formation and resorption also plays an important role in the overall Pi (and also Ca^{2+}) homeostasis. A higher deposition of Pi in the bone could also contribute to the absence of hyperphosphatemia in the GABARAP$^{-/-}$ mice. Therefore, I analyzed the Pi and Ca^{2+} content in bones (femur as well as lumbar vertebrae

L3 and L4) from GABARAP$^{+/+}$ and GABARAP$^{-/-}$ mice. As shown in figure 19, the Pi and the Ca^{2+} content was similar in lumbar vertebrae and in femurs of GABARAP$^{+/+}$ and GABARAP$^{-/-}$ mice.

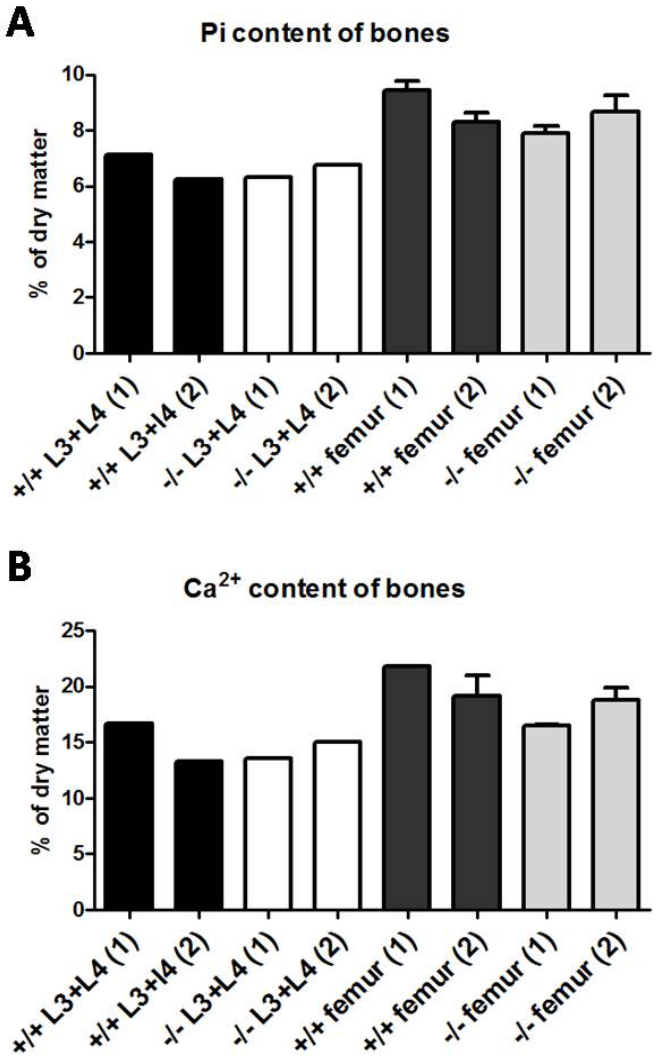

Figure 19: Pi and Ca^{2+} content of the bones of GABARAP$^{+/+}$ and GABARAP$^{-/-}$ mice.

Bone ashes were obtained from the lumbar vertebras L3 and L4 as well as from the femurs of 2 GABARAP$^{+/+}$ and 2 GABARAP$^{-/-}$ mice. Pi and Ca^{2+} content were determined by colorimetric assays. Each column represents either L3+L4 or the femur of one animal.

6.3 Regulation of NaPi-IIa in GABARAP$^{-/-}$ mice

6.3.1 PTH-induced internalization in GABARAP$^{-/-}$ mice

To test whether the downregulation of NaPi-IIa in response to PTH is affected by the loss of GABARAP, we injected animals with PTH and quantified the amount of NaPi-IIa remaining in renal BBM 45 minutes after injection. Based on immunoblot data, administration of PTH led to ~50 % reduction of NaPi-IIa in BBM of GABARAP$^{+/+}$ mice (Fig. 20A). PTH also induced a reduction of NaPi-IIa in GABARAP$^{-/-}$ mice. Moreover, despite the higher basal levels in GABARAP$^{-/-}$ animals, the amount of NaPi-IIa remaining upon PTH administration was similar in both groups of mice (Fig. 20A).

I then analyzed the Pi transport activity into BBMV isolated from control and PTH-injected GABARAP$^{+/+}$ and GABARAP$^{-/-}$ mice. In agreement with the immunoblot data, Na^+-dependent uptakes of ^{32}Pi decreased upon PTH treatment. Furthermore, similar uptakes were measured in BBMV isolated from both groups of animals upon PTH treatment, despite the higher basal uptake measured in mutant mice (Fig. 20B).

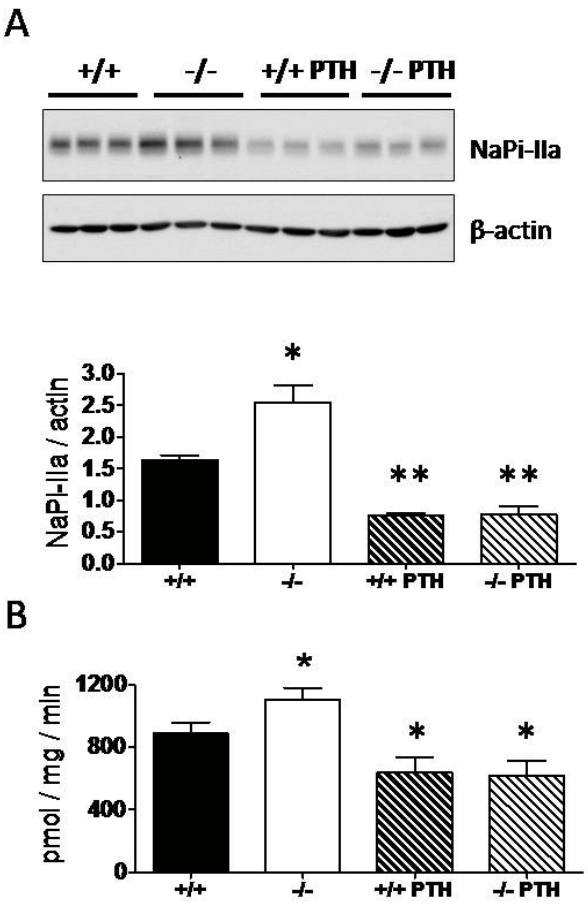

Figure 20: PTH-induced endocytosis of NaPi-IIa in GABARAP$^{+/+}$ and GABARAP$^{-/-}$ mice.

(A) Representative Immunoblot of NaPi-IIa on BBM isolated from GABARAP$^{+/+}$ and GABARAP$^{-/-}$ mice injected with either saline or PTH. Expression was normalized to β-actin for the quantification. Similar results were obtained in six animals per group. **(B)** Na^+-dependent uptake of P_i into BBMV isolated from kidneys of GABARAP$^{-/-}$ and GABARAP$^{+/+}$ mice injected with saline or PTH (n=6). Uptakes were analyzed after 1 minute incubation as indicated. Data are means ± SEM. (* $p \leq 0.05$, ** $p \leq 0.01$, unpaired student t-test; relative to GABARAP$^{+/+}$ injected with saline).

6.3.2 Adaptation of GABARAP$^{-/-}$ mice to chronic alterations of dietary Pi

In order to study whether the absence of GABARAP interferes with the chronic adaptation to the dietary Pi content, we fed GABARAP$^{+/+}$ and GABARAP$^{-/-}$ mice with either a high (1.2%) or low (0.1%) Pi diet for 5 days. Urinary Pi excretion, serum Pi concentration, NaPi-IIa and NaPi-IIc expression as well as localization and Pi transport activity were analyzed in these animals.

6.3.2.1 Urinary and serum Pi concentrations

First, urinary Pi excretion was determined. Both in GABARAP$^{+/+}$ and GABARAP$^{-/-}$ mice the high Pi diet resulted in an increased excretion of Pi in the urine as compared with the low Pi chow (Fig. 21A). Under high Pi conditions urinary Pi excretion was similar in GABARAP$^{+/+}$ and GABARAP$^{-/-}$ mice. However, urinary Pi excretion was even smaller in GABARAP$^{-/-}$ than in GABARAP$^{+/+}$ mice when animals were fed with a low Pi diet.

Serum Pi levels were then compared in these four groups of mice (Fig. 20B). In contrast to the urinary Pi excretion, serum Pi levels were similar in the groups that received a high and a low Pi diet. Moreover, the levels of Pi in serum were also comparable in GABARAP$^{+/+}$ and GABARAP$^{-/-}$ mice.

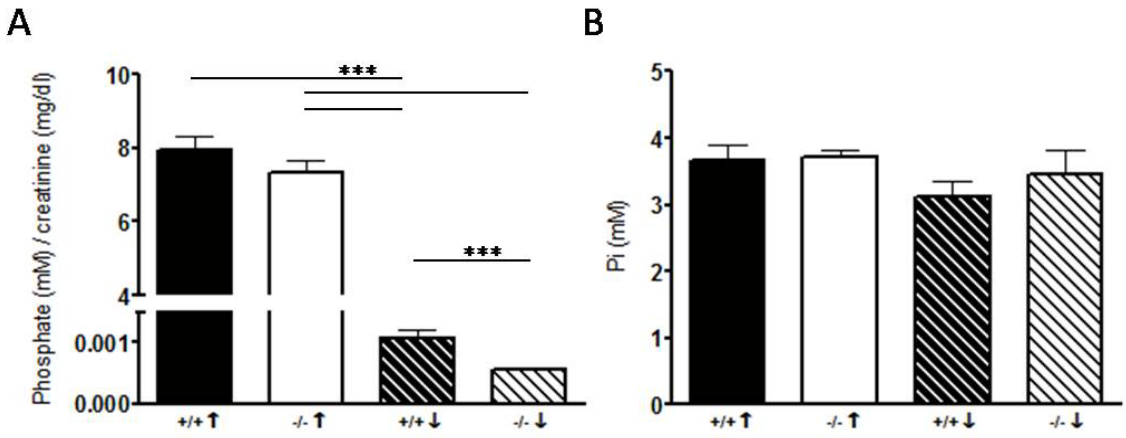

Figure 21: Chronic adaptation to a high or low dietary Pi content.

(A) Urinary Pi excretion as a ratio to urinary creatinine in GABARAP$^{+/+}$ and GABARAP$^{-/-}$ mice fed with either a high (↑) or a low (↓) Pi diet for 5 days (n=6). **(B)** Serum Pi concentration in the same animals. Data are means ± SEM. (*** $p \leq 0.001$, unpaired student t-test)

6.3.2.2 NaPi-IIa and NaPi-IIc expression

In a next step, I determined the effect of the high /low Pi diets on the expression of NaPi-IIa and NaPi-IIc in renal BBM (Fig. 22A). A high dietary Pi intake led to a decreased abundance of both transporters as compared to a low dietary Pi intake. This reduction was observed in GABARAP$^{+/+}$ as well as in GABARAP$^{-/-}$ mice. NaPi-IIa expression was similar in GABARAP$^{+/+}$ and in GABARAP$^{-/-}$ mice fed with a high Pi diet. However, the expression of NaPi-IIa was greater in GABARAP$^{-/-}$ than in GABARAP$^{+/+}$ mice when the animals received a low Pi chow. This is in agreement with the reduced urinary excretion of Pi in GABARAP$^{-/-}$ mice under this dietary condition (Fig. 21A). The expression and adaptation of NaPi-IIc was similar in GABARAP$^{+/+}$ and GABARAP$^{-/-}$ animals.

In addition to the protein levels, mRNA abundance of both transporters was determined by Real-Time PCR. As shown in Fig. 22B NaPi-IIa mRNA expression was similar in all groups suggesting that dietary adaptation of NaPi-IIa involves posttranscriptional mechanisms. NaPi-IIc mRNA levels were increased in mice fed with a low Pi diet as compared to those that were given a high Pi diet. This increase was observed both in GABARAP$^{+/+}$ and GABARAP$^{-/-}$ mice.

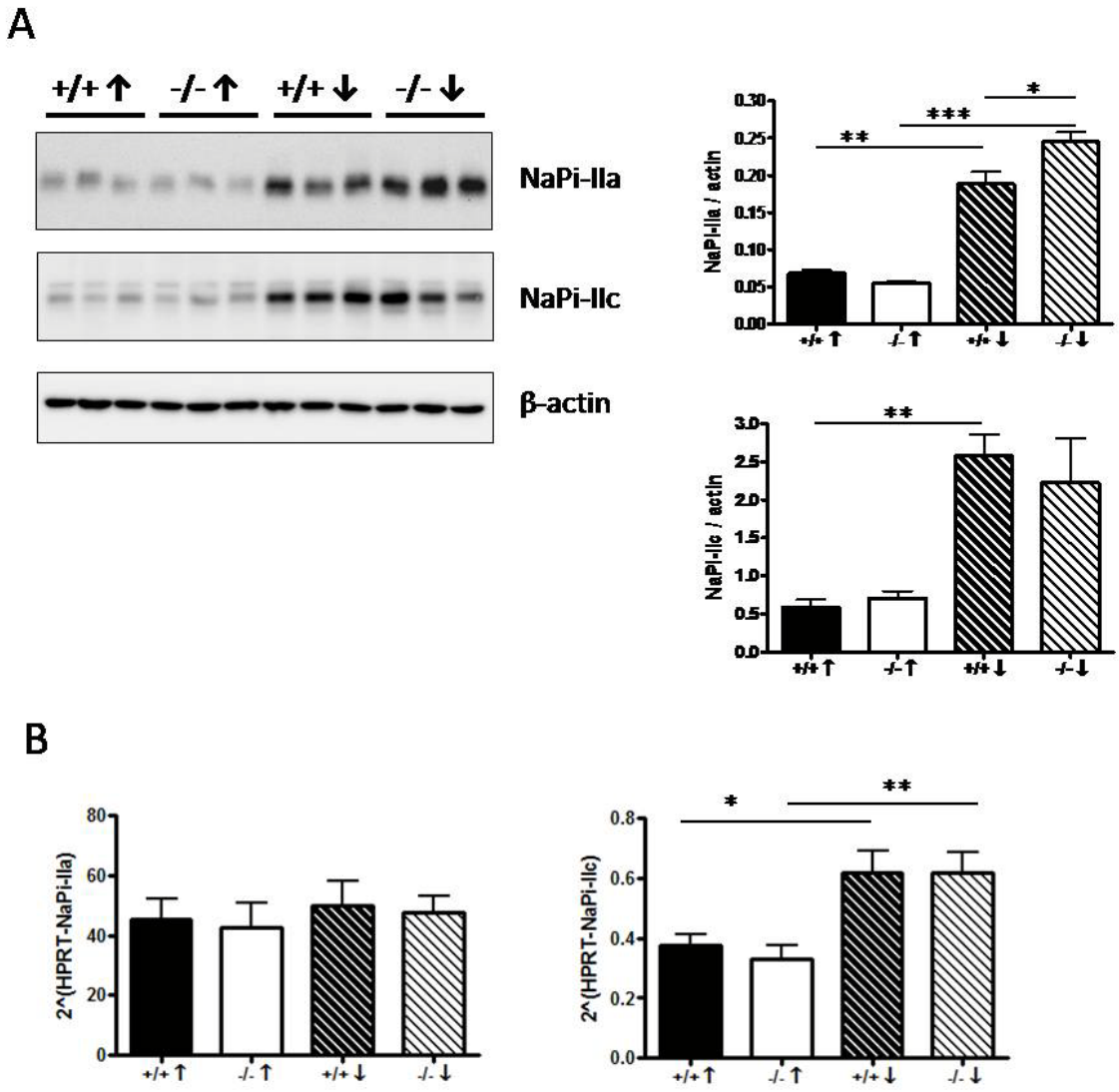

Figure 22: Expression of NaPi-IIa and NaPi-IIc in mice adapted to chronic high/low dietary Pi.

(A) Representative Immunoblot of NaPi-IIa and NaPi-IIc on BBM isolated from GABARAP$^{+/+}$ and GABARAP$^{-/-}$ mice fed with either a high (↑) or a low (↓) Pi diet. Expression was normalized to β-actin for the quantification. Similar results were obtained in six animals per group. **(B)** Real-Time PCR to determine NaPi-IIa (left) and NaPi-IIc (right) mRNA levels normalized to HPRT (n=6). Data are means ± SEM. (* $p \leq 0.05$; ** $p \leq 0.01$, unpaired student t-test)

In agreement with the Immunoblot data (Fig. 22) the low Pi diet increased the immunofluorescence signal of NaPi-IIa and NaPi-IIc in kidney slices. However, GABARAP$^{+/+}$ and GABARAP$^{-/-}$ mice displayed the same subcellular pattern and distribution of NaPi-IIa and NaPi-IIc along the nephron segments both under chronic low or high Pi intake (Fig. 23).

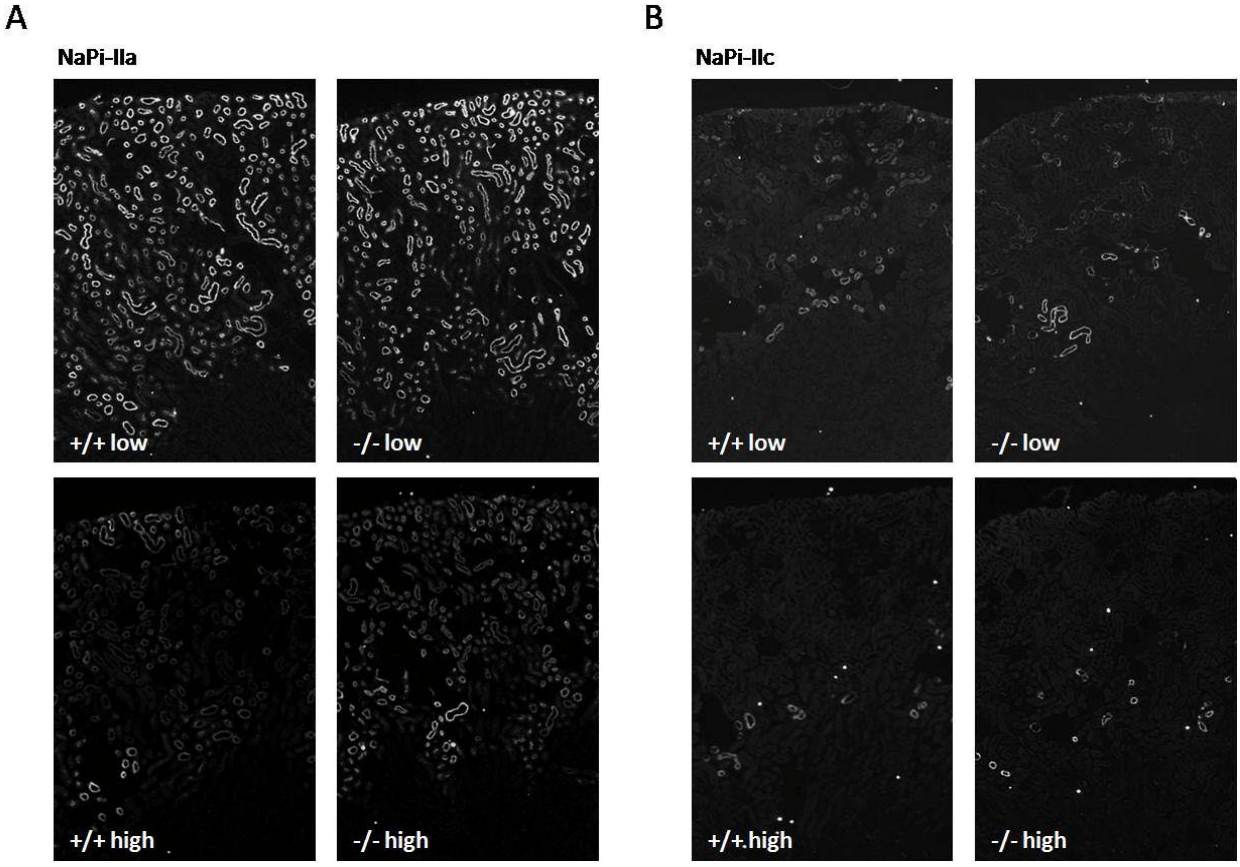

Figure 23: Localization of NaPi-IIa and NaPi-IIc after chronic adaptation to a high or low Pi diet.

Immunostaining of **(A)** NaPi-IIa and **(B)** NaPi-IIc on kidney cryosections obtained from GABARAP$^{+/+}$ (left) and GABARAP$^{-/-}$ mice (right). Upper panels show cryosections from mice fed with a low Pi diet. Lower panels show cryosections from mice fed with a high Pi diet. Renal cortical overviews are displayed as grayscale figure.

6.3.2.3 Pi Transport activity

Based on the immunoblot and immunohistochemistry data the dietary Pi content is a prominent regulator of NaPi-IIa and NaPi-IIc expression. In addition, the loss of GABARAP causes a more pronounced upregulation of NaPi-IIa when mice are fed with a low Pi diet (Fig. 22A). In order to determine whether the detected protein levels correlate with Pi transport activity, we analyzed the Pi uptake into renal BBMV isolated from the same mice (Fig. 24). Uptake of ^{32}Pi into BBMV was significantly smaller in the groups that were fed with a high Pi diet than in those mice fed with a low Pi chow. No difference between GABARAP$^{+/+}$ and GABARAP$^{-/-}$ mice was observed under a high Pi diet. When

fed with a low Pi diet, uptake into GABARAP$^{-/-}$ BBMV tended to be bigger than in GABARAP$^{+/+}$, but the difference was just below statistical significance (p=0.054).

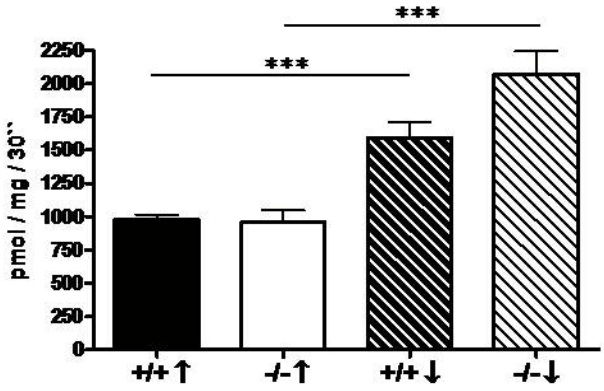

Figure 24: Na$^+$-dependent ^{32}P uptake into renal BBMV after chronic adaptation to a high or a low Pi diet.

Na$^+$-dependent uptake of P_i into BBMV isolated from kidneys of GABARAP$^{+/+}$ and GABARAP$^{-/-}$ fed with either a high (↑) or a low (↓) Pi diet (n=6). Uptakes were analyzed after 30 seconds incubation as indicated. Data are means ± SEM. (* p ≤ 0.05, unpaired student t-test)

6.3.3 Adaptation of GABARAP$^{-/-}$ mice to acute switches of dietary Pi

To study if the acute adaptation to the dietary content of Pi is affected by the absence of GABARAP the effect of rapid switches of the diet was analyzed.

6.3.3.1 Switch from low to high Pi diet

Mice were fed with a low Pi diet for 5 days. On day 5, the mice were either kept on low Pi diet or were switched to a high Pi diet for four hours. Urinary Pi excretion, serum Pi concentration and NaPi-IIa expression were analyzed in these animals.

First, urinary Pi excretion was determined. The switch to a high Pi diet resulted in an increased excretion of Pi in the urine as compared with the urine of those animals that stayed with the low Pi diet (Fig. 25A). This adaptation was observed both in GABARAP$^{+/+}$ and in GABARAP$^{-/-}$ mice. Although urinary Pi

excretion tended to be smaller in GABARAP$^{-/-}$ than in GABARAP$^{+/+}$ mice the difference was not significant.

Serum Pi levels were compared in these animals as shown in figure 25B. In contrast to chronic adaptation (Fig. 21B), an acute change in dietary Pi intake leads to changes in serum Pi concentrations. Mice that were switched from a low to a high Pi diet had significantly higher serum Pi levels compared to the groups that were kept on low Pi diet. No difference between GABARAP$^{+/+}$ and GABARAP$^{-/-}$ mice was observed with regard to the serum Pi levels.

Mice that were switched to a high Pi diet displayed a significantly reduced abundance of NaPi-IIa compared to those animals that were kept on the low Pi chow (Fig. 25C). This rapid downregulation of NaPi-IIa was not affected by the absence of GABARAP since NaPi-IIa expression was comparable between GABARAP$^{+/+}$ and GABARAP$^{-/-}$ mice. Surprisingly, under these dietary condition (2 hrs feeding period per day) the levels of NaPi-IIa were similar in GABARAP$^{-/-}$ and in GABARAP$^{+/+}$ mice.

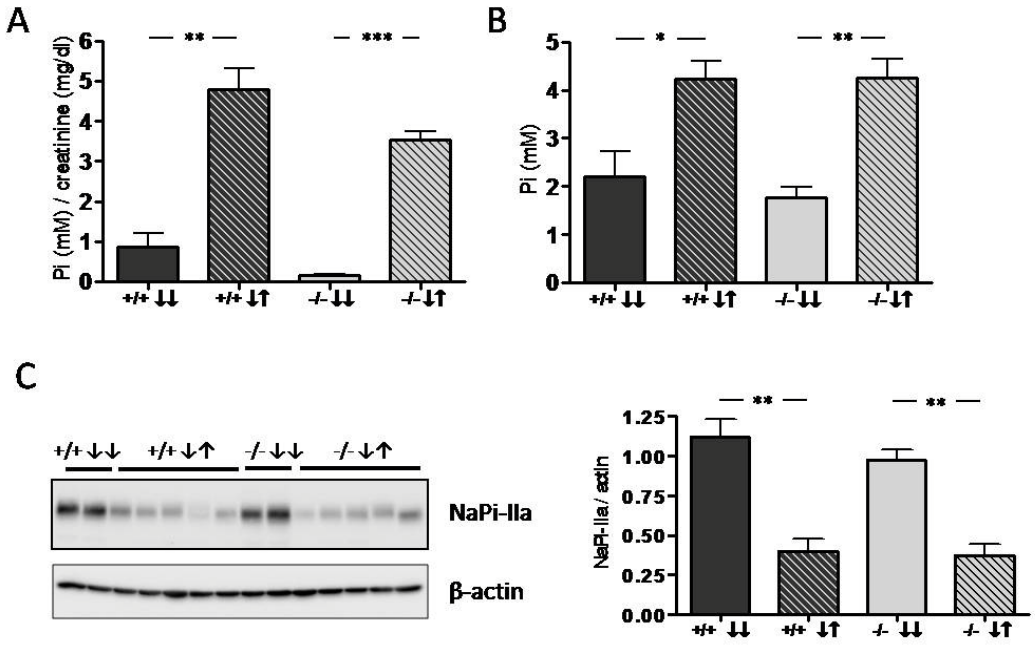

Figure 25: Acute switch from a low to a high Pi diet.

(A) Urinary Pi excretion as a ratio to urinary creatinine in GABARAP$^{+/+}$ and GABARAP$^{-/-}$ mice fed with a low Pi diet (↓↓) for 5 days (n=3) compared to animals that were fed with a low Pi diet for 5 days and then swiched to a high Pi diet (↓↑) for four hours (n=5). **(B)** Serum Pi concentration in the same animals. **(C)** Representative Immunoblot of NaPi-IIa on BBM of the same animals. Expression was normalized to β-actin for the quantification. Data are means ± SEM. (*p ≤ 0.05, **p ≤ 0.01, *** p ≤ 0.001, unpaired student t-test)

6.3.3.2 Switch from high to low Pi diet

GABARAP$^{+/+}$ and GABARAP$^{-/-}$ mice were fed with a high Pi diet for 5 days. On the last day, some animals were kept on a high Pi chow whereas others were switched to low Pi diet for four hours. Urinary Pi excretion, serum Pi concentration and NaPi-IIa expression were determined.

Mice that were switched to a low Pi diet displayed a significantly decreased urinary Pi excretion than those that still received the high Pi chow (Fig. 26A). However, there was no difference between GABARAP$^{+/+}$ and GABARAP$^{-/-}$ mice in any of the two dietary conditions.

As indicated above for the acute high to low Pi diet switch, also the acute low to high adaptaion caused alterations of the serum Pi concentrations. The mice that were acutely switched to a low Pi diet had significantly lower serum Pi levels than mice that were kept on high Pi diet (Fig. 26B). No difference between GABARAP$^{+/+}$ and GABARAP$^{-/-}$ mice was observed with regard to the serum Pi levels.

Mice switched to a low Pi diet on the last day of the experiment had a higher NaPi-IIa abundance than those that still got the high Pi diet (Fig. 26C). Upregulation of NaPi-IIa was similar in GABARAP$^{+/+}$ and GABARAP$^{-/-}$ mice. As for the opposite acute switch, the basal expression of NaPi-IIa was similar in GABARAP$^{+/+}$ and GABARAP$^{-/-}$ mice, possibly due to the reduced food intake during the 2 hrs feeding period.

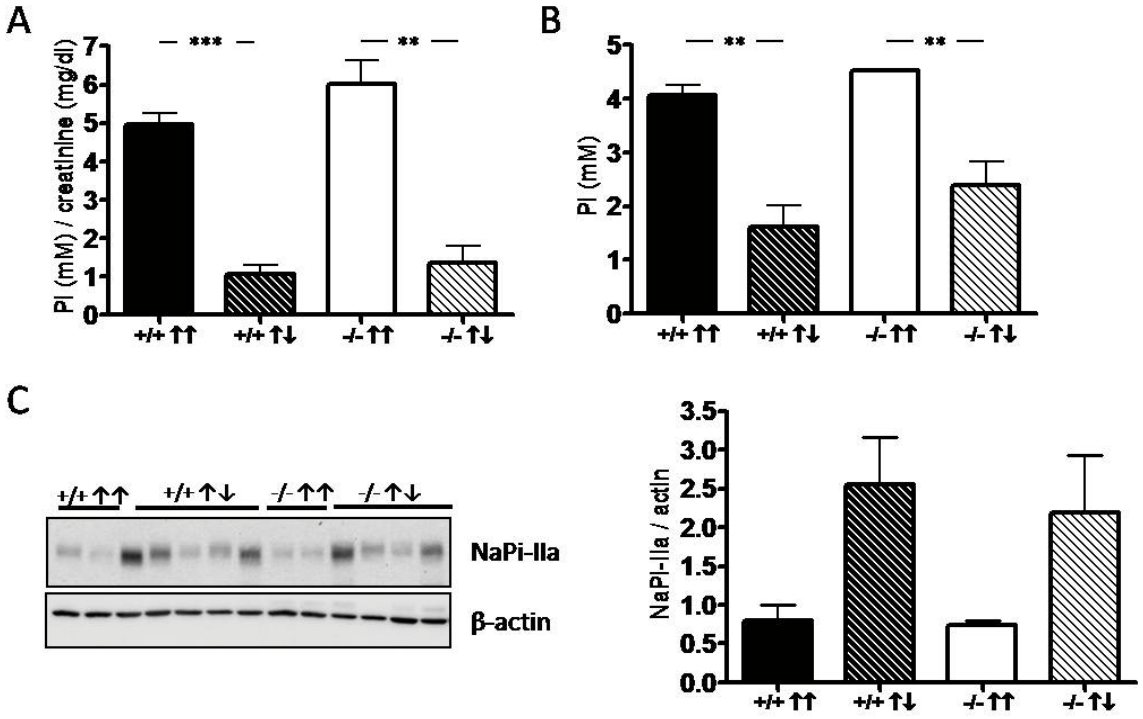

Figure 26: Acute switch from a high to a low Pi diet.

(A) Urinary Pi excretion as a ratio to urinary creatinine in GABARAP$^{+/+}$ and GABARAP$^{-/-}$ mice fed with a high Pi diet (↑↑) for 5 days (n=3) compared to animals that were fed with a high Pi diet for 5 days and then swiched to a low Pi diet (↑↓) for four hours (n=5). **(B)** Serum Pi concentration in the same animals. **(C)** Representative Immunoblot of NaPi-IIa on BBM of the same animals. Expression was normalized to β-actin for the quantification. Data are means ± SEM. (**p ≤ 0.01, *** p ≤ 0.001, unpaired student t-test)

7. Discussion

Renal Pi reabsorption is mainly determined by the expression of NaPi-IIa in the BBM of proximal tubules in mice. Apical positioning and membrane abundance of NaPi-IIa depends on a network of interacting proteins. In a membrane yeast-two-hybrid screen using the functional cotransporter lacking the previously identified C-terminal PDZ-binding motif as bait, GABARAP was found as a putative novel interacting partner of NaPi-IIa. Therefore, the first aim of this study was to confirm the interaction between NaPi-IIa and GABARAP. In a next step the physiological role of the interaction between GABARAP and NaPi-IIa was studied in a GABARAP$^{-/-}$ mouse model.

7.1 Renal expression of GABARAP

GABARAP mRNA has been previously shown to be expressed in various tissues, including the kidneys (Xin, Yu et al. 2001). However, no detailed information regarding the mRNA distribution within the kidney was available. Therefore, I performed Real-Time PCR analysis on RNA isolated from dissected murine nephrons. GABARAP mRNA was detected in all tested segments along the nephron at similar, relatively high expression levels. In order to rule out cross-contaminations with mRNA from different nephron segments, I additionally analyzed the expression profile of marker genes which are known to be differentially expressed along the nephron. NaPi-IIa was chosen as a marker for proximal tubules. Its mRNA has been shown to be highly abundant in proximal convoluted tubules (S1 and S2) and to be expressed to a lesser extend also in S3 segments (Madjdpour, Bacic et al. 2004). NaPi-IIa mRNA is absent in the more distal tubule (Custer, Meier et al. 1993). Using β-ENaC as a second marker, I was aiming to demonstrate the enrichment of distal nephron segments. β-ENaC mRNA is present in the distal concoluted tubule, the cortical collecting duct (CCD) and the outer medullary collecting ducts (Vehaskari, Hempe et al. 1998). For both markers, we could detect the mRNA only in those nephrons in which their expression has been described earlier. Therefore, it is unlikely that the uniform GABARAP mRNA

distribution along the nephron is due to segments cross-contamination. Importantly for our study, GABARAP mRNA expression was detected in proximal convoluted and proximal straight tubules, those segments where NaPi-IIa mRNA is also present.

Endogenous GABARAP protein expression has been reported in rat brain, liver, kidney, spleen, skeletal muscle and heart (Tanida, Ueno et al. 2004) as well as in various human cell lines (Green, O'Hare et al. 2002). Immunoblot using an antibody raised against human GABARAP (Green, O'Hare et al. 2002) confirmed its expression in murine BBM preparations. In addition to the band at the expected molecular weight of 17 kDa a second product of faster mobility was detected. This second product has been suggested to represent a lipidated form of GABARAP (Tanida, Ueno et al. 2004). Both bands were specific to GABARAP as indicated by their absence in BBM preparations from GABARAP$^{-/-}$ mice.

GABARAP immunostainings show a punctate distribution within the cytoplasm of breast epithelial cells, HeLa cells and neurons (Wang, Bedford et al. 1999; Kneussel, Haverkamp et al. 2000; Green, O'Hare et al. 2002; Klebig, Seitz et al. 2005). Interestingly, GABARAP does not co-localize with the γ2-subunit of $GABA_A$-receptors or with gephyrin in mouse retina sections (Kneussel, Haverkamp et al. 2000). Unfortunately, our attempts to identify the localization of GABARAP in the kidney failed, since similar signals were detected in cryosections from GABARAP$^{+/+}$ and GABARAP$^{-/-}$ kidneys (data not shown). These signals could represent either non-specific binding of the antibody to renal tissue or cross-reaction with the GABARAP-like proteins GABARAPL1 and GABARAPL2. Both paralogs are expressed in kidney, albeit at very low levels (Sagiv, Legesse-Miller et al. 2000; Wang, Dun et al. 2006). Despite this technical caveat, the presence of GABARAP in BBM preparations points to a subcellular proximity of GABARAP and NaPi-IIa, making the interaction between both proteins plausible.

7.2 Interaction between GABARAP and NaPi-IIa

The interaction of GABARAP and NaPi-IIa was verified by GST-pull downs and by co-immunoprecipitation from transfected HEK293 cells. Taken together, these data suggest that NaPi-IIa and GABARAP associate *in vitro* and may also interact with each other *in vivo*. Furthermore, the sites involved in the protein-protein interation were partially characterized. It has been reported that the association of GABARAP with the γ-subunit of $GABA_A$-receptors depends on a region between the amino acids 36-68 of GABARAP (Wang, Bedford et al. 1999). In order to find the molecular determinant of GABARAP that mediates the interaction with NaPi-IIa, we expressed two overlapping halves of GABARAP (aa 1-68 and aa 37-117, respectively) fused to GST as described (Wang, Bedford et al. 1999). Both fusion proteins were capable of pulling down NaPi-IIa from BBM, suggesting that similar to the $GABA_A$-receptor γ-subunit the interaction of GABARAP with NaPi-IIa involves the region between the amino acids 36-68 of GABARAP. GABARAP 36-117 has been shown to interact also with the transferrin receptor (Green, O'Hare et al. 2002). Therefore, these internal residues might represent a common motif for protein-protein interactions.

Recently, a consensus sequence for GABARAP-binding was proposed based on the binding sites of calreticulin, clathrin heavy chain as well as the γ2-subunit of the $GABA_A$ receptor. This consensus sequence contains few amino acids that surround a highly conserved tryptophan residue. These residues interact with a hydrophobic patch on the surface of GABARAP (Thielmann, Mohrluder et al. 2008). We identified a sequence that would fit to this motif in the C-terminus of NaPi-IIa. Therefore, pull downs were performed with lysates from HEK293 cells transfected either with the full length or a truncated cotransporter (Δ571) which lacks the tryptophan-containing peptide. Both the full length and the truncated NaPi-IIa were pulled down by GST-GABARAP. Although these data does not rule out its potential implication *in vivo*, it suggests that the mentioned C-terminal peptide of NaPi-IIa is not required for the *in vitro* interaction with GABARAP. Since pull-down experiments using discrete intracellular domains of NaPi-IIa failed and I was unable to identify conditions which allow the expression of membrane domains of NaPi-IIa

in E.coli or cultured cells, the domain of NaPi-IIa that mediates the interaction with GABARAP remains elusive.

7.3 Metabolic characterization of GABARAP$^{-/-}$ mice

The generation of GABARAP$^{-/-}$ mice by gene trap methodology has been described (O'Sullivan, Kneussel et al. 2005). It was reported that these animals show a normal phenotype with regard to the expression of $GABA_A$ receptor γ2-subunit in synapses. The lack of a phenotype for the $GABA_A$ receptor expression in inhibitory synapses in the brain is in conflict with results obtained in *in vitro* studies in which overexpression of GABARAP increased the membrane abundance of $GABA_A$ receptors (Chen, Wang et al. 2000; Leil, Chen et al. 2004; Chen, Chang et al. 2007). This discrepancy has been attributed to a compensatory effect of GABARAPL1 and/or GABARAPL2 in mice. In particular GABARAPL2 has also been shown to interact with the $GABA_A$ receptor and tubulin (Mansuy, Boireau et al. 2004). These studies were performed only with regard to the $GABA_A$ receptor expression in the brain. The GABARAP$^{-/-}$ mice were not further characterized justifying a detailed study of their metabolic status.

GABARAP$^{-/-}$ mice had a higher body weight as compared to GABARAP$^{+/+}$ mice of a the same age. This increased body weight of is not due to a higher dietary intake, since GABARAP$^{-/-}$ and GABARAP$^{+/+}$ animals consumed similar amounts of food. I observed a higher fat content in the abdomen of GABARAP$^{-/-}$ mice compared to GABARAP$^{+/+}$ mice while harvesting the kidneys, but I did not perform further studies with regard to the differences in body weight.

GABARAP$^{-/-}$ mice drank less water as compared to GABARAP$^{+/+}$ mice. In a recent report the interaction between GABARAP and the angiotensin II type I receptor has been described. Similar to the findings concerning the $GABA_A$ receptor, overexpression of GABARAP increased the surface expression of the angiotensin II type I receptor in cells (Cook, Re et al. 2008). As angiotensin II acts on the hypothalamus to increase the sensation of thirst (Boron and Boulpaep 2005), the lack of GABARAP might influence the drinking behavior of

GABARAP$^{-/-}$ mice. The reduced intake of water in the mutant mice translated in a reduced urinary output. The excreted urine of GABARAP$^{-/-}$ mice displayed an increased osmolarity and also a higher creatinine concentration. Urine concentration and dilution is mainly mediated by regulation of Aquaporin 2 water channels in the apical membrane of principal cells of the collecting tubules and ducts (Boron and Boulpaep 2005). Regulation of Aquaporin 2 occurs at the transcriptional and posttranscriptional level (Deen, Verdijk et al. 1994). In an attempt to investigate the reduced urinary output of GABARAP$^{-/-}$ mice in further detail, I determined AQP2 mRNA levels in kidneys isolated from GABARAP$^{-/-}$ and GABARAP$^{+/+}$ mice by Real-Time PCR. When normalized to HPRT mRNA expression, AQP2 mRNA levels were similar in GABARAP$^{+/+}$ and GABARAP$^{-/-}$ mice (data not shown). This suggests that the absence of GABARAP does not induce changes of AQP2 mRNA.

The rationale of our study was to investigate, whether the interaction with GABARAP influences the membrane expression of NaPi-IIa and thus renal handling of Pi. Therefore, I compared the urinary Pi excretion of GABARAP$^{-/-}$ and GABARAP$^{+/+}$ mice. In these experiments, the urinary creatinine concentration was used to normalize for the different urinary volume excreted by both groups. We found that urinary Pi excretion was significantly reduced in GABARAP$^{-/-}$ as compared to GABARAP$^{+/+}$ mice. This reduced excretion was specifically found for Pi, since the excretion of all other tested ions was comparable in both groups after normalization to urinary creatinine.

Interestingly, the serum concentration of Pi was similar in GABARAP$^{+/+}$ and GABARAP$^{-/-}$ mice. Whether this is related to a higher metabolic consumption of Pi in GABARAP$^{-/-}$ mice, due for instance to their higher body weight, or to some compensatory mechanism(s) such as reduced intestinal absorption or enhanced bone deposition will be discussed later (section 7.5). Interestingly, the Ca^{2+} concentration in blood was also similar in both groups of animals. This is important, since plasma Ca^{2+} regulates PTH secretion by the parathyroid gland in a negative feedback loop (Boron and Boulpaep 2005). Since serum Ca^{2+} and Pi concentrations were both unchanged, serum PTH levels might be similar in GABARAP$^{+/+}$ and GABARAP$^{-/-}$ animals. Unfortunately, this remains speculative, since our attempts to measure serum PTH levels failed due to a lack of sensitivity of the assay. The PTH receptor belongs to the

family of G-protein coupled receptors and it signals via G_s and $G_{q/i,o}$ as indicated before. Therefore binding of PTH leads to intracellular accumulation of cAMP and Ca^{2+}. We measured the concentration of cAMP in the urine and found no difference between GABARAP$^{+/+}$ and GABARAP$^{-/-}$ mice suggesting that the basal cAMP status is similar in both groups of animals.

In summary, the changes in urinary Pi excretion validated a study of a potential role of GABARAP in NaPi-IIa expression and regulation

7.4 NaPi-IIa abundance and activity in GABARAP$^{-/-}$ mice under normal conditions

Urinary excretion of Pi is mostly controlled by the rate of reabsorption in the proximal tubule (Forster, Hernando et al. 2006). NaPi-IIa is believed to be the main Na-dependent Pi cotransporter in mice based on the severe renal wasting phenotype of NaPi-IIa$^{-/-}$ mice (Beck, Karaplis et al. 1998) as well as on RNA hybrid depletion experiments (Segawa, Kaneko et al. 2002). NaPi-IIc was considered to play only a minor role. However, mutations of NaPi-IIc were recently identified in families with several hypophosphatemic syndromes (Bergwitz, Roslin et al. 2006; Ichikawa, Sorenson et al. 2006; Lorenz-Depiereux, Benet-Pages et al. 2006). Thus, either renal Pi reabsorption differs greatly between human and mice or the renal Pi handling is still not understood completely.

Therefore, I next analyzed whether the reduced urinary excretion of Pi detected in GABARAP$^{-/-}$ mice was due to changes on the expression of NaPi-IIa. In addition, I also analyzed the expression of NaPi-IIc. I found that NaPi-IIa (but not NaPi-IIc) abundance was significantly increased in renal BBM of GABARAP$^{-/-}$ as compared to GABARAP$^{+/+}$ mice. Furthermore, the increased NaPi-IIa membrane abundance was reflected by a higher Na-dependent Pi transport activity across the BBM as demonstrated by uptake experiments. These results are in line with the reduced urinary Pi excretion of GABARAP$^{-/-}$ mice. Thus, the absence of GABARAP leads to upregulation of surface-expressed NaPi-IIa. In contrast to this effect on NaPi-IIa, overexpression of GABARAP in different cell lines was previously shown to increase the

membrane abundance of the $GABA_A$ receptor as well as the angiotensin II type I receptor (Leil, Chen et al. 2004; Cook, Re et al. 2008). It was concluded from these data that GABARAP acts as a general trafficking protein along the biosynthetic pathway which increases the membrane abundance of its interacting membrane partners. However, as mentioned before, no phenotype with regard to the $GABA_A$ receptors has been observed in $GABARAP^{-/-}$ mice (O'Sullivan, Kneussel et al. 2005). This disagreement between *in vivo* and *in vitro* studies could be due to a compensatory mechanism in the *in vivo* studies or to inadecuate cellular models in the *in vitro* studies. Alternatively, despite its ability to interact with various membrane proteins through a common motif, GABARAP might exert different effects on the respective interacting partner. This could depend on the tissue-specific expression of a certain set of interacting proteins that form the network in which the membrane protein is embedded.

Interestingly, the crystal-structure of GABARAP revealed the presence of a motif which resembles an ubiquitin-like fold (Bavro, Sola et al. 2002). Furthermore, it has been shown that GABARAP can be processed by a set of E1- and E2-like enzymes in a similar way than ubiquitin (Tanida, Ueno et al. 2004). At the end of this ubiquitin-like processing, GABARAP is conjugated to phospholipids rather than to proteins (Sou, Tanida et al. 2006). This mechanism has only been studied *in vitro*. The impact of membrane conjugation of GABARAP on the expression/stability of membrane proteins such as NaPi-IIa remains to be established.

Another mechanism to explain the increased NaPi-IIa abundance in BBM is the upregulation of its important scaffolding protein NHERF1. Studies in OK cells have shown that the apical expression of NaPi-IIa decreases when its association with NHERF1 is prevented (Hernando, Deliot et al. 2002). Furthermore, $NHERF1^{-/-}$ mice show a reduced expression of NaPi-IIa in the proximal BBM associated with higher intracellular levels (Shenolikar, Voltz et al. 2002). Thus, we can speculate that increased amounts of NHERF1 might result in a higher surface expression of NaPi-IIa. Indeed higher levels of NHERF1 were detected in kidneys of $GABARAP^{-/-}$ mice. However, the mechanism underlying the upregulation of NHERF1 in the absence of GABARAP remains to be addressed in further studies.

Changes on NaPi-IIa abundance in response to acute stimuli are due to regulated insertion/retrieval from the BBM rather than to changes on mRNA levels (Levi, Lotscher et al. 1994; Forster, Hernando et al. 2006) whereas chronic adaptation to dietary Pi may (Levi, Lotscher et al. 1994) or may not involve transcriptional regulation (Madjdpour, Bacic et al. 2004). Therefore, we quantified the amount of NaPi-IIa mRNA in kidneys from GABARAP$^{+/+}$ and GABARAP$^{-/-}$ mice by Real-Time PCR. NaPi-IIa mRNA expression levels were comparable in both groups of animals. Therefore, upregulation of the cotransporter in GABARAP$^{-/-}$ mice is most likely due to posttranscriptional mechanisms. As reported previously (Madjdpour, Bacic et al. 2004), the expression of NaPi-IIc mRNA was very low as compared to NaPi-IIa and its levels were similar in GABARAP$^{+/+}$ and GABARAP$^{-/-}$ kidneys.

In summary, these data suggest that under normal conditions GABARAP plays a suppressive role in the expression/stabilization of NaPi-IIa in renal proximal tubules and its absence cannot be compensated by GABARAP-like paralogs as it has been proposed for the expression of $GABA_A$ receptors (O'Sullivan, Kneussel et al. 2005).

7.5 Pi homeostasis in GABARAP$^{-/-}$ mice under normal conditions

Despite the reduced urinary excretion of Pi (associated with higher NaPi-IIa levels), GABARAP$^{-/-}$ mice have normal circulating levels of this element, suggesting the presence of a compensatory mechanism that prevents the animals from becoming hyperphosphatemic. Pi homeostasis is achieved by a coordinated absorption of Pi from the diet and renal Pi excretion. In addition, bone formation and resorption can help to maintain serum Pi levels in a constant millimolar range.

Pi absorption from the diet occurs in the small intestine in a Na-dependent as well as in a Na-independent manner. In contrast to the Na-dependent transport of Pi across the membrane, Na-independent Pi transport is not regulated (Lee, Walling et al. 1986). In mice, NaPi-IIb is expressed in the luminal membrane of enterocytes and is considered to be the main NaPi cotransporter in the small intestine (Hilfiker, Hattenhauer et al. 1998).

In mice, NaPi-IIb expression is highest in the ileum and only little amounts are found in other segments such as duodenum and jejunum (Marks, Srai et al. 2006). Although intestinal Pi absorption is not regulated in response to acute stimulus, chronic situations such as a prolonged intake of a low Pi diet lead to adaptive changes of NaPi-IIb (Hattenhauer, Traebert et al. 1999; Radanovic, Wagner et al. 2005). Experiments in *Xenopus laevis* oocytes suggest that in contrast to NaPi-IIa, regulation of NaPi-IIb involves ubiquitination by the ubiquitin-ligase Nedd4-2 which is in turn regulated through its phosphorylation by the Serum and Glucocorticoid-Inducible kinase 1 (SGK1) (Palmada, Dieter et al. 2004). NaPi-IIb abundance was significantly decreased in the BBM of the ileum of GABARAP$^{-/-}$ compared to GABARAP$^{+/+}$ mice. A decreased intestinal Pi absorption could act as compensatory mechanism in order to balance the hypophosphaturia observed in GABARAP$^{-/-}$ mice. However, it remains to be established whether this decreased abundance of the cotransporter correlates with a lower intestinal Pi absorption in GABARAP$^{-/-}$ mice and what is the mechanism underlying this finding. In preliminary experiments using GST-GABARAP in order to pull down NaPi-IIb from intestinal BBM, no evidence for a direct interaction between GABARAP and NaPi-IIb could be obtained (data not shown). Pi absorption in the small intestine is influenced by the active vitamin D metabolite 1,25-dihydroxyvitamin D_3. Higher 1,25-dihydroxyvitamin D_3 levels increase the abundance of NaPi-IIb protein in the BBM (Hattenhauer, Traebert et al. 1999; Xu, Bai et al. 2002). Increase of active 1,25-dihydroxyvitamin D_3 occurs via stimulation of the renal 25-hydroxyvitamin-D_3-1α-hydroxylase. Control of the 25-hydroxyvitamin-D_3-1α-hydroxylase takes place at the level of its mRNA (Wu, Finch et al. 1996; Brown, Dusso et al. 1999). Interestingly, renal 25-hydroxyvitamin-D_3-1α-hydroxylase mRNA levels were reduced in GABARAP$^{-/-}$ mice (data not shown). Taken together, these findings suggest that the lower NaPi-IIb abundance in the absence of GABARAP is a compensatory mechanism that is independent on a physical interaction between NaPi-IIb and GABARAP. Instead it might be achieved by reduced levels of 1,25-dihydroxyvitamin D_3, although this remains to be proved.

As mentioned before, Pi (as hydroxyapatite) is an essential component of the mineralized bone matrix. The bone is a dynamic tissue which is constantly

built by osteoblasts and resorbed by osteoclasts. Several NaPi-cotransporters including PiT-1, PiT-2 (Nielsen, Pedersen et al. 2001) as well as NaPi-IIa and NaPi-IIb (Lundquist, Murer et al. 2007) have been shown to be expressed in cultured osteoblast-like cells. Na-dependent Pi transport into osteoblast-like cells has been reported to be modulated by PTH (Selz, Caverzasio et al. 1989) as well as by the presence of extracellular Pi (Lundquist, Murer et al. 2007). NaPi-IIa and PiT-1 expression have been also reported in cultured osteoclast cells (Gupta, Guo et al. 1997; Gupta, Tenenhouse et al. 2001). Furthermore, the number of osteoclasts is decreased in young NaPi-IIa$^{-/-}$ mice (Gupta, Tenenhouse et al. 2001), but the bone content of Pi was not determined. In order to test whether the loss of GABARAP affects the Pi and Ca^{2+} content in bone, we analyzed bone ashes from GABARAP$^{+/+}$ and GABARAP$^{-/-}$ mice. The content of both major bone components was similar in both groups.

Taken together, our data indicate that the reduced intestinal absorption may compensate for the increased renal Pi reabsorption in GABARAP$^{-/-}$ mice without an apparent involvement of the skeleton.

7.6 Regulation of NaPi-IIa by PTH in GABARAP$^{-/-}$ mice

As discussed above, GABARAP$^{-/-}$ mice show higher levels of NaPi-IIa in renal BBM together with a higher expression of NHERF1. In principle, upregulation of NaPi-IIa on steady-state conditions could be due to an increased rate of membrane insertion, reduced membrane removal or changes on membrane stability. Therefore I analyzed the behavior of NaPi-IIa in response to maneuvers that control (acutely/chronically) the removal and membrane insertion of the cotransporter.

PTH is a potent phosphaturic hormone which causes the internalization of NaPi-IIa. As described before, rapid internalization of NaPi-IIa in response to PTH occurs most likely via the pathway of receptor-mediated endocytosis (Kempson, Helmle et al. 1990; Bacic, Lehir et al. 2006). This pathway involves clathrin-coated vesicles which fuse with the early endosomes. An interaction between the clathrin heavy chain and GABARAP has been reported (Mohrluder, Hoffmann et al. 2007), but the physiological relevance of this interaction has not

been addressed. I analyzed whether PTH-induced downregulation of NaPi-IIa is affected by the lack of GABARAP. NaPi-IIa downregulation in response to PTH was not impaired in GABARAP$^{-/-}$ mice and, despite a higher basal abundance of NaPi-IIa, expression levels after PTH-injections were reduced to similar levels in GABARAP$^{+/+}$ and GABARAP$^{-/-}$ mice. These data indicate that the higher basal NaPi-IIa levels can not be explained by a decreased responsiveness for PTH in GABARAP$^{-/-}$ mice.

7.7 Dietary regulation of NaPi-IIa in GABARAP$^{-/-}$ mice

Changes in the dietary intake of Pi affect the renal Pi excretion by adjusting the amount of NaPi-IIa in the apical microvilli. The expression of NaPi-IIa in the BBM increases in response to a low dietary intake of Pi, whereas in conditions of high dietary Pi the level of NaPi-IIa decreases (Biber, Hernando et al. 2008). Both responses are fast and can be detected few hours (acute adaptation) after Pi ingestion (Levine, Ho et al. 1986). Acute downregulation of NaPi-IIa relays on its endocytic retrieval and lysosomal degradation, similar to the PTH effect (Keusch, Traebert et al. 1998). Acute upregulation does not require *de novo* synthesis; instead it depends on an intact microtubular cytoskeleton, suggesting the sorting of intracellularly stored NaPi-IIa to the BBM. Neither acute upregulation nor acute downregulation of NaPi-IIa was impaired in GABARAP$^{-/-}$ mice. These data suggest that the acute dietary regulation of NaPi-IIa does not require the presence of GABARAP. Furthermore, together with the PTH data, it suggests that at least the regulated membrane retrieval/insertion of NaPi-IIa is not impaired in the absence of GABARAP.

The capacity of renal Pi reabsorption remains adjusted even during prolonged intake of dietary Pi (Levi, Kempson et al. 1996). This regulation involves post-transcriptional mechanisms for NaPi-IIa whereas NaPi-IIc mRNA levels are elevated under a prolonged low Pi diet. As for PTH, NaPi-IIa is downregulated to similar levels in GABARAP$^{-/-}$ and GABARAP$^{+/+}$ mice chronically fed with a high Pi diet. In contrast, NaPi-IIa (but not NaPi-IIc) abundance is higher in GABARAP$^{-/-}$ than in GABARAP$^{+/+}$ mice chronically fed with a low Pi diet, similar to the findings reported for a normal dietary Pi intake. Changes of GABARAP

abundance (or differentially lipidation) were not observed in the BBM under all dietary feeding conditions (data not shown).

In summary, NaPi-IIa expression is reduced to similar levels in GABARAP$^{+/+}$ and GABARAP$^{-/-}$ mice by phosphaturic factors (PTH and high Pi diet). In contrast, NaPi-IIa is greater in GABARAP$^{-/-}$ than in GABRAP$^{+/+}$ both in the absence of phosphaturic stimulus (normal diet) and under Pi conserving settings (low Pi diet). The greater than normal upregulation of NaPi-IIa in response to a low Pi diet is observed after a chronic but not with an acute feeding. Taken together these data suggest that GABARAP exerts its effect on NaPi-IIa neither in the biosynthetic nor in the degradative pathway, but instead negatively influences NaPi-IIa basal turnover/half-life *in vivo.*

8. Future perspectives

In this study, a novel interacting partner of NaPi-IIa, GABARAP, was identified and GABARAP$^{-/-}$ mice were initially characterized with regard to Pi homeostasis. In these studies a number of interesting aspects were discovered which should be addressed in further studies:

a. To fully understand the function of GABARAP in the kidney, it would be important to determine its (subcellular) localization. For this purpose, a new antibody of sufficient quality would have to be raised and tested.

b. The establishment of a cell culture model with a stable knock-down of GABARAP would help to analyze the effect on NaPi-IIa. This cell culture model would allow the clarification of the molecular mechanism that underlies the increased NaPi-IIa abundance in GABARAP$^{-/-}$ mice. In particular, we could test in this model whether GABARAP indeed interferes with the basal turnover/half life of NaPi-IIa.

c. GST-pull down did not provide evidence for a direct interaction between GABARAP and NHERF1. Therefore, it remains to be clarified how the lack of GABARAP increases NHERF1 expression in mice. Furthermore, it would be of interest to investigate whether the elevated NHERF1 abundance itself causes the increased NaPi-IIa BBM expression in GABARAP$^{-/-}$ mice (e.g. GABARAP$^{-/-}$/NHERF1$^{-/-}$ mice)

d. We show that the intestinal NaPi-IIb cotransporter is downregulated in GABARAP$^{-/-}$ mice. Further studies should address whether the decreased NaPi-IIb abundance in the intestinal BBM correlates with a reduced Pi absorption from the diet. As for NHERF1, no interaction between GABARAP and NaPi-IIb could be identified so far. Therefore, it would be important to understand whether this is indeed only a compensatory effect and how it is achieved.

e. Various factors influence Pi homeostasis among them PTH, vitamin D, insulin, growth hormones, steroid hormones and FGF23. The knowledge of the abundance of these factors in GABARAP$^{-/-}$ mice would allow not only further clarification of the phenotype of these mice but could also allow the identification of patients with a similar phenotype. Eventually, it could be tested whether there are patients with mutations in the GABARAP gene.

9. References

Bacic, D., M. Lehir, et al. (2006). "The renal Na+/phosphate cotransporter NaPi-IIa is internalized via the receptor-mediated endocytic route in response to parathyroid hormone." Kidney Int **69**(3): 495-503.

Bacic, D., N. Schulz, et al. (2003). "Involvement of the MAPK-kinase pathway in the PTH-mediated regulation of the proximal tubule type IIa Na+/Pi cotransporter in mouse kidney." Pflugers Arch **446**(1): 52-60.

Bavro, V. N., M. Sola, et al. (2002). "Crystal structure of the GABA(A)-receptor-associated protein, GABARAP." EMBO Rep **3**(2): 183-9.

Beck, L., A. C. Karaplis, et al. (1998). "Targeted inactivation of Npt2 in mice leads to severe renal phosphate wasting, hypercalciuria, and skeletal abnormalities." Proc Natl Acad Sci U S A **95**(9): 5372-7.

Bellocchio, E. E., R. J. Reimer, et al. (2000). "Uptake of glutamate into synaptic vesicles by an inorganic phosphate transporter." Science **289**(5481): 957-60.

Bergwitz, C., N. M. Roslin, et al. (2006). "SLC34A3 mutations in patients with hereditary hypophosphatemic rickets with hypercalciuria predict a key role for the sodium-phosphate cotransporter NaPi-IIc in maintaining phosphate homeostasis." Am J Hum Genet **78**(2): 179-92.

Biber, J., M. Custer, et al. (1993). "Localization of NaPi-1, a Na/Pi cotransporter, in rabbit kidney proximal tubules. II. Localization by immunohistochemistry." Pflugers Arch **424**(3-4): 210-5.

Biber, J., N. Hernando, et al. (2008). "Regulation of phosphate transport in proximal tubules." Pflugers Arch.

Biber, J., B. Stieger, et al. (1981). "A high yield preparation for rat kidney brush border membranes. Different behaviour of lysosomal markers." Biochim Biophys Acta **647**(2): 169-76.

Biber, J., B. Stieger, et al. (2007). "Isolation of renal proximal tubular brush-border membranes." Nat Protoc **2**(6): 1356-9.

Boron, W. F. and E. L. Boulpaep (2005). Medical physiology: a cellular and molecular approach, Elsevier Saunders.

Breusegem, S. Y., N. Halaihel, et al. (2005). "Acute and chronic changes in cholesterol modulate Na-Pi cotransport activity in OK cells." Am J Physiol Renal Physiol **289**(1): F154-65.

Brown, A. J., A. Dusso, et al. (1999). "Vitamin D." Am J Physiol **277**(2 Pt 2): F157-75.

Busch, A. E., A. Schuster, et al. (1996). "Expression of a renal type I sodium/phosphate transporter (NaPi-1) induces a conductance in Xenopus oocytes permeable for organic and inorganic anions." Proc Natl Acad Sci U S A **93**(11): 5347-51.

Capuano, P., D. Bacic, et al. (2007). "Defective coupling of apical PTH receptors to phospholipase C prevents internalization of the Na+-phosphate cotransporter NaPi-IIa in Nherf1-deficient mice." Am J Physiol Cell Physiol **292**(2): C927-34.

Capuano, P., D. Bacic, et al. (2005). "Expression and regulation of the renal Na/phosphate cotransporter NaPi-IIa in a mouse model deficient for the PDZ protein PDZK1." Pflugers Arch **449**(4): 392-402.

Chen, L., H. Wang, et al. (2000). "The gamma-aminobutyric acid type A (GABAA) receptor-associated protein (GABARAP) promotes GABAA receptor clustering and modulates the channel kinetics." Proc Natl Acad Sci U S A **97**(21): 11557-62.

Chen, Z. W., C. S. Chang, et al. (2007). "C-terminal modification is required for GABARAP-mediated GABA(A) receptor trafficking." J Neurosci **27**(25): 6655-63.

Chien, M. L., E. O'Neill, et al. (1998). "Phosphate depletion enhances the stability of the amphotropic murine leukemia virus receptor mRNA." Virology **240**(1): 109-17.

Collins, J. F., L. Bai, et al. (2004). "The SLC20 family of proteins: dual functions as sodium-phosphate cotransporters and viral receptors." Pflugers Arch **447**(5): 647-52.

Cook, J. L., R. N. Re, et al. (2008). "The trafficking protein GABARAP binds to and enhances plasma membrane expression and function of the angiotensin II type 1 receptor." Circ Res **102**(12): 1539-47.

Coyle, J. E. and D. B. Nikolov (2003). "GABARAP: lessons for synaptogenesis." Neuroscientist **9**(3): 205-16.

Custer, M., M. Lotscher, et al. (1994). "Expression of Na-P(i) cotransport in rat kidney: localization by RT-PCR and immunohistochemistry." Am J Physiol **266**(5 Pt 2): F767-74.

Custer, M., F. Meier, et al. (1993). "Localization of NaPi-1, a Na-Pi cotransporter, in rabbit kidney proximal tubules. I. mRNA localization by reverse transcription/polymerase chain reaction." Pflugers Arch **424**(3-4): 203-9.

Dawson, T. P., R. Gandhi, et al. (1989). "Ecto-5'-nucleotidase: localization in rat kidney by light microscopic histochemical and immunohistochemical methods." J Histochem Cytochem **37**(1): 39-47.

Deen, P. M., M. A. Verdijk, et al. (1994). "Requirement of human renal water channel aquaporin-2 for vasopressin-dependent concentration of urine." Science **264**(5155): 92-5.

Deliot, N., N. Hernando, et al. (2005). "Parathyroid hormone treatment induces dissociation of type IIa Na+-P(i) cotransporter-Na+/H+ exchanger regulatory factor-1 complexes." Am J Physiol Cell Physiol **289**(1): C159-67.

Fakitsas, P., G. Adam, et al. (2007). "Early aldosterone-induced gene product regulates the epithelial sodium channel by deubiquitylation." J Am Soc Nephrol **18**(4): 1084-92.

Forster, I. C., N. Hernando, et al. (2006). "Proximal tubular handling of phosphate: A molecular perspective." Kidney Int **70**(9): 1548-59.

Forster, I. C., K. Kohler, et al. (2002). "Forging the link between structure and function of electrogenic cotransporters: the renal type IIa Na+/Pi cotransporter as a case study." Prog Biophys Mol Biol **80**(3): 69-108.

Forster, I. C., D. D. Loo, et al. (1999). "Stoichiometry and Na+ binding cooperativity of rat and flounder renal type II Na+-Pi cotransporters." Am J Physiol **276**(4 Pt 2): F644-9.

Fukumoto, S. and T. Yamashita (2002). "Fibroblast growth factor-23 is the phosphaturic factor in tumor-induced osteomalacia and may be phosphatonin." Curr Opin Nephrol Hypertens **11**(4): 385-9.

Gisler, S. M., S. Kittanakom, et al. (2008). "Monitoring protein-protein interactions between the mammalian integral membrane transporters and PDZ-interacting partners using a modified split-ubiquitin membrane yeast two-hybrid system." Mol Cell Proteomics.

Gisler, S. M., C. Madjdpour, et al. (2003). "PDZK1: II. an anchoring site for the PKA-binding protein D-AKAP2 in renal proximal tubular cells." Kidney Int **64**(5): 1746-54.

Gisler, S. M., S. Pribanic, et al. (2003). "PDZK1: I. a major scaffolder in brush borders of proximal tubular cells." Kidney Int **64**(5): 1733-45.

Gisler, S. M., I. Stagljar, et al. (2001). "Interaction of the type IIa Na/Pi cotransporter with PDZ proteins." J Biol Chem **276**(12): 9206-13.

Goetz, R., A. Beenken, et al. (2007). "Molecular insights into the klotho-dependent, endocrine mode of action of fibroblast growth factor 19 subfamily members." Mol Cell Biol **27**(9): 3417-28.

Green, F., T. O'Hare, et al. (2002). "Association of human transferrin receptor with GABARAP." FEBS Lett **518**(1-3): 101-6.

Gupta, A., X. L. Guo, et al. (1997). "Regulation of sodium-dependent phosphate transport in osteoclasts." J Clin Invest **100**(3): 538-49.

Gupta, A., H. S. Tenenhouse, et al. (2001). "Identification of the type II Na(+)-Pi cotransporter (Npt2) in the osteoclast and the skeletal phenotype of Npt2-/- mice." Bone **29**(5): 467-76.

Hattenhauer, O., M. Traebert, et al. (1999). "Regulation of small intestinal Na-P(i) type IIb cotransporter by dietary phosphate intake." Am J Physiol **277**(4 Pt 1): G756-62.

Hernando, N., N. Deliot, et al. (2002). "PDZ-domain interactions and apical expression of type IIa Na/P(i) cotransporters." Proc Natl Acad Sci U S A **99**(18): 11957-62.

Hilfiker, H., O. Hattenhauer, et al. (1998). "Characterization of a murine type II sodium-phosphate cotransporter expressed in mammalian small intestine." Proc Natl Acad Sci U S A **95**(24): 14564-9.

Hisano, S., H. Haga, et al. (1997). "Immunohistochemical and RT-PCR detection of Na+-dependent inorganic phosphate cotransporter (NaPi-2) in rat brain." Brain Res **772**(1-2): 149-55.

Ichikawa, S., A. H. Sorenson, et al. (2006). "Intronic deletions in the SLC34A3 gene cause hereditary hypophosphatemic rickets with hypercalciuria." J Clin Endocrinol Metab **91**(10): 4022-7.

Ito, M., S. Iidawa, et al. (2004). "Interaction of a farnesylated protein with renal type IIa Na/Pi co-transporter in response to parathyroid hormone and dietary phosphate." Biochem J **377**(Pt 3): 607-16.

Karim-Jimenez, Z., N. Hernando, et al. (2000). "A dibasic motif involved in parathyroid hormone-induced down-regulation of the type IIa NaPi cotransporter." Proc Natl Acad Sci U S A **97**(23): 12896-901.

Karim-Jimenez, Z., N. Hernando, et al. (2001). "Molecular determinants for apical expression of the renal type IIa Na+/Pi-cotransporter." Pflugers Arch **442**(5): 782-90.

Kavanaugh, M. P., D. G. Miller, et al. (1994). "Cell-surface receptors for gibbon ape leukemia virus and amphotropic murine retrovirus are inducible sodium-dependent phosphate symporters." Proc Natl Acad Sci U S A **91**(15): 7071-5.

Kempson, S. A., C. Helmle, et al. (1990). "Parathyroid hormone action on phosphate transport is inhibited by high osmolality." Am J Physiol **258**(5 Pt 2): F1336-44.

Keusch, I., M. Traebert, et al. (1998). "Parathyroid hormone and dietary phosphate provoke a lysosomal routing of the proximal tubular Na/Pi-cotransporter type II." Kidney Int **54**(4): 1224-32.

Kido, S., K. Miyamoto, et al. (1999). "Identification of regulatory sequences and binding proteins in the type II sodium/phosphate cotransporter NPT2 gene responsive to dietary phosphate." J Biol Chem **274**(40): 28256-63.

Kittler, J. T., P. Rostaing, et al. (2001). "The subcellular distribution of GABARAP and its ability to interact with NSF suggest a role for this protein in the intracellular transport of GABA(A) receptors." Mol Cell Neurosci **18**(1): 13-25.

Klebig, C., S. Seitz, et al. (2005). "Characterization of {gamma}-aminobutyric acid type A receptor-associated protein, a novel tumor suppressor, showing reduced expression in breast cancer." Cancer Res **65**(2): 394-400.

Kneussel, M., S. Haverkamp, et al. (2000). "The gamma-aminobutyric acid type A receptor (GABAAR)-associated protein GABARAP interacts with gephyrin but is not involved in receptor anchoring at the synapse." Proc Natl Acad Sci U S A **97**(15): 8594-9.

Kocher, O., N. Comella, et al. (1998). "Identification and partial characterization of PDZK1: a novel protein containing PDZ interaction domains." Lab Invest **78**(1): 117-25.

Kurosu, H., Y. Ogawa, et al. (2006). "Regulation of fibroblast growth factor-23 signaling by klotho." J Biol Chem **281**(10): 6120-3.

Lanaspa, M. A., H. Giral, et al. (2007). "Interaction of MAP17 with NHERF3/4 induces translocation of the renal Na/Pi IIa transporter to the trans-Golgi." Am J Physiol Renal Physiol **292**(1): F230-42.

Lee, D. B., M. W. Walling, et al. (1986). "Phosphate transport across rat jejunum: influence of sodium, pH, and 1,25-dihydroxyvitamin D3." Am J Physiol **251**(1 Pt 1): G90-5.

Leil, T. A., Z. W. Chen, et al. (2004). "GABAA receptor-associated protein traffics GABAA receptors to the plasma membrane in neurons." J Neurosci **24**(50): 11429-38.

Levi, M., S. A. Kempson, et al. (1996). "Molecular regulation of renal phosphate transport." J Membr Biol **154**(1): 1-9.

Levi, M., M. Lotscher, et al. (1994). "Cellular mechanisms of acute and chronic adaptation of rat renal P(i) transporter to alterations in dietary P(i)." Am J Physiol **267**(5 Pt 2): F900-8.

Levine, B. S., L. D. Ho, et al. (1986). "Renal adaptation to phosphorus deprivation: characterization of early events." J Bone Miner Res **1**(1): 33-40.

Liesegang, A., L. Loch, et al. (2005). "Influence of phytase added to a vegetarian diet on bone metabolism in pregnant and lactating sows." J Anim Physiol Anim Nutr (Berl) **89**(3-6): 120-8.

Lorenz-Depiereux, B., A. Benet-Pages, et al. (2006). "Hereditary hypophosphatemic rickets with hypercalciuria is caused by mutations in the sodium-phosphate cotransporter gene SLC34A3." Am J Hum Genet **78**(2): 193-201.

Lundquist, P., H. Murer, et al. (2007). "Type II Na+-Pi cotransporters in osteoblast mineral formation: regulation by inorganic phosphate." Cell Physiol Biochem **19**(1-4): 43-56.

Madjdpour, C., D. Bacic, et al. (2004). "Segment-specific expression of sodium-phosphate cotransporters NaPi-IIa and -IIc and interacting proteins in mouse renal proximal tubules." Pflugers Arch **448**(4): 402-10.

Magagnin, S., A. Werner, et al. (1993). "Expression cloning of human and rat renal cortex Na/Pi cotransport." Proc Natl Acad Sci U S A **90**(13): 5979-83.

Mahon, M. J., M. Donowitz, et al. (2002). "Na(+)/H(+) exchanger regulatory factor 2 directs parathyroid hormone 1 receptor signalling." Nature **417**(6891): 858-61.

Mansuy, V., W. Boireau, et al. (2004). "GEC1, a protein related to GABARAP, interacts with tubulin and GABA(A) receptor." Biochem Biophys Res Commun **325**(2): 639-48.

Marks, J., S. K. Srai, et al. (2006). "Intestinal phosphate absorption and the effect of vitamin D: a comparison of rats with mice." Exp Physiol **91**(3): 531-7.

McWilliams, R. R., S. Y. Breusegem, et al. (2005). "Shank2E binds NaP(i) cotransporter at the apical membrane of proximal tubule cells." Am J Physiol Cell Physiol **289**(4): C1042-51.

Medici, D., M. S. Razzaque, et al. (2008). "FGF-23-Klotho signaling stimulates proliferation and prevents vitamin D-induced apoptosis." J Cell Biol **182**(3): 459-65.

Mohrluder, J., Y. Hoffmann, et al. (2007). "Identification of clathrin heavy chain as a direct interaction partner for the gamma-aminobutyric acid type A receptor associated protein." Biochemistry **46**(50): 14537-43.

Murer, H., I. Forster, et al. (2004). "The sodium phosphate cotransporter family SLC34." Pflugers Arch **447**(5): 763-7.

Nielsen, L. B., F. S. Pedersen, et al. (2001). "Expression of type III sodium-dependent phosphate transporters/retroviral receptors mRNAs during osteoblast differentiation." Bone **28**(2): 160-6.

Nowik, M., N. Picard, et al. (2008). "Renal phosphaturia during metabolic acidosis revisited: molecular mechanisms for decreased renal phosphate reabsorption." Pflugers Arch.

O'Sullivan, G. A., M. Kneussel, et al. (2005). "GABARAP is not essential for GABA receptor targeting to the synapse." Eur J Neurosci **22**(10): 2644-8.

Ohkido, I., H. Segawa, et al. (2003). "Cloning, gene structure and dietary regulation of the type-IIc Na/Pi cotransporter in the mouse kidney." Pflugers Arch **446**(1): 106-15.

Palmada, M., M. Dieter, et al. (2004). "Regulation of intestinal phosphate cotransporter NaPi IIb by ubiquitin ligase Nedd4-2 and by serum- and glucocorticoid-dependent kinase 1." Am J Physiol Gastrointest Liver Physiol **287**(1): G143-50.

Pribanic, S., S. M. Gisler, et al. (2003). "Interactions of MAP17 with the NaPi-IIa/PDZK1 protein complex in renal proximal tubular cells." Am J Physiol Renal Physiol **285**(4): F784-91.

Radanovic, T., C. A. Wagner, et al. (2005). "Regulation of intestinal phosphate transport. I. Segmental expression and adaptation to low-P(i) diet of the type IIb Na(+)-P(i) cotransporter in mouse small intestine." Am J Physiol Gastrointest Liver Physiol **288**(3): G496-500.

Razzaque, M. S. (2008). "FGF23-mediated regulation of systemic phosphate homeostasis: is klotho an essential player?" Am J Physiol Renal Physiol.

Reczek, D., M. Berryman, et al. (1997). "Identification of EBP50: A PDZ-containing phosphoprotein that associates with members of the ezrin-radixin-moesin family." J Cell Biol **139**(1): 169-79.

Sagiv, Y., A. Legesse-Miller, et al. (2000). "GATE-16, a membrane transport modulator, interacts with NSF and the Golgi v-SNARE GOS-28." EMBO J **19**(7): 1494-504.

Segawa, H., I. Kaneko, et al. (2002). "Growth-related renal type II Na/Pi cotransporter." J Biol Chem **277**(22): 19665-72.

Segawa, H., E. Kawakami, et al. (2003). "Effect of hydrolysis-resistant FGF23-R179Q on dietary phosphate regulation of the renal type-II Na/Pi transporter." Pflugers Arch **446**(5): 585-92.

Segawa, H., A. Onitsuka, et al. (2009). "Type IIc sodium-dependent phosphate transporter regulates calcium metabolism." J Am Soc Nephrol **20**(1): 104-13.

Segawa, H., S. Yamanaka, et al. (2005). "Internalization of renal type IIc Na-Pi cotransporter in response to a high-phosphate diet." Am J Physiol Renal Physiol **288**(3): F587-96.

Segawa, H., S. Yamanaka, et al. (2007). "Correlation between hyperphosphatemia and type II Na-Pi cotransporter activity in klotho mice." Am J Physiol Renal Physiol **292**(2): F769-79.

Selz, T., J. Caverzasio, et al. (1989). "Regulation of Na-dependent Pi transport by parathyroid hormone in osteoblast-like cells." Am J Physiol **256**(1 Pt 1): E93-100.

Shenolikar, S., J. W. Voltz, et al. (2002). "Targeted disruption of the mouse NHERF-1 gene promotes internalization of proximal tubule sodium-phosphate cotransporter type IIa and renal phosphate wasting." Proc Natl Acad Sci U S A **99**(17): 11470-5.

Shimada, T., M. Kakitani, et al. (2004). "Targeted ablation of Fgf23 demonstrates an essential physiological role of FGF23 in phosphate and vitamin D metabolism." J Clin Invest **113**(4): 561-8.

Sou, Y. S., I. Tanida, et al. (2006). "Phosphatidylserine in addition to phosphatidylethanolamine is an in vitro target of the mammalian Atg8 modifiers, LC3, GABARAP, and GATE-16." J Biol Chem **281**(6): 3017-24.

Stagljar, I., C. Korostensky, et al. (1998). "A genetic system based on split-ubiquitin for the analysis of interactions between membrane proteins in vivo." Proc Natl Acad Sci U S A **95**(9): 5187-92.

Stubbs, J., S. Liu, et al. (2007). "Role of fibroblast growth factor 23 in phosphate homeostasis and pathogenesis of disordered mineral metabolism in chronic kidney disease." Semin Dial **20**(4): 302-8.

Takeda, E., H. Yamamoto, et al. (2004). "Inorganic phosphate homeostasis and the role of dietary phosphorus." J Cell Mol Med **8**(2): 191-200.

Tanida, I., M. Komatsu, et al. (2003). "GATE-16 and GABARAP are authentic modifiers mediated by Apg7 and Apg3." Biochem Biophys Res Commun **300**(3): 637-44.

Tanida, I., T. Ueno, et al. (2004). "LC3 conjugation system in mammalian autophagy." Int J Biochem Cell Biol **36**(12): 2503-18.

Tenenhouse, H. S., J. Martel, et al. (2003). "Differential effects of Npt2a gene ablation and X-linked Hyp mutation on renal expression of Npt2c." Am J Physiol Renal Physiol **285**(6): F1271-8.

Tenenhouse, H. S. and Y. Sabbagh (2002). "Novel phosphate-regulating genes in the pathogenesis of renal phosphate wasting disorders." Pflugers Arch **444**(3): 317-26.

Thielmann, Y., J. Mohrluder, et al. (2008). "An indole-binding site is a major determinant of the ligand specificity of the GABA type A receptor-associated protein GABARAP." Chembiochem **9**(11): 1767-75.

Traebert, M., H. Volkl, et al. (2000). "Luminal and contraluminal action of 1-34 and 3-34 PTH peptides on renal type IIa Na-P(i) cotransporter." Am J Physiol Renal Physiol **278**(5): F792-8.

Vehaskari, V. M., J. M. Hempe, et al. (1998). "Developmental regulation of ENaC subunit mRNA levels in rat kidney." Am J Physiol **274**(6 Pt 1): C1661-6.

Vernier-Magnin, S., S. Muller, et al. (2001). "A novel early estrogen-regulated gene gec1 encodes a protein related to GABARAP." Biochem Biophys Res Commun **284**(1): 118-25.

Wang, H., F. K. Bedford, et al. (1999). "GABA(A)-receptor-associated protein links GABA(A) receptors and the cytoskeleton." Nature **397**(6714): 69-72.

Wang, H. and R. W. Olsen (2000). "Binding of the GABA(A) receptor-associated protein (GABARAP) to microtubules and microfilaments suggests involvement of the cytoskeleton in GABARAPGABA(A) receptor interaction." J Neurochem **75**(2): 644-55.

Wang, Y., S. L. Dun, et al. (2006). "Distribution and ultrastructural localization of GEC1 in the rat CNS." Neuroscience **140**(4): 1265-76.

Weinman, E. J., R. S. Biswas, et al. (2007). "Parathyroid hormone inhibits renal phosphate transport by phosphorylation of serine 77 of sodium-hydrogen exchanger regulatory factor-1." J Clin Invest **117**(11): 3412-20.

Weinman, E. J., A. Boddeti, et al. (2003). "NHERF-1 is required for renal adaptation to a low-phosphate diet." Am J Physiol Renal Physiol **285**(6): F1225-32.

Weinman, E. J., C. Minkoff, et al. (2000). "Signal complex regulation of renal transport proteins: NHERF and regulation of NHE3 by PKA." Am J Physiol Renal Physiol **279**(3): F393-9.

Weinman, E. J., D. Steplock, et al. (2003). "NHERF-1 uniquely transduces the cAMP signals that inhibit sodium-hydrogen exchange in mouse renal apical membranes." FEBS Lett **536**(1-3): 141-4.

Werner, A., L. Dehmelt, et al. (1998). "Na+-dependent phosphate cotransporters: the NaPi protein families." J Exp Biol **201**(Pt 23): 3135-42.

Wu, S., J. Finch, et al. (1996). "Expression of the renal 25-hydroxyvitamin D-24-hydroxylase gene: regulation by dietary phosphate." Am J Physiol **271**(1 Pt 2): F203-8.

Xin, Y., L. Yu, et al. (2001). "Cloning, expression patterns, and chromosome localization of three human and two mouse homologues of GABA(A) receptor-associated protein." Genomics **74**(3): 408-13.

Xu, H., L. Bai, et al. (2002). "Age-dependent regulation of rat intestinal type IIb sodium-phosphate cotransporter by 1,25-(OH)(2) vitamin D(3)." Am J Physiol Cell Physiol **282**(3): C487-93.

Zambrowicz, B. P., G. A. Friedrich, et al. (1998). "Disruption and sequence identification of 2,000 genes in mouse embryonic stem cells." Nature **392**(6676): 608-11.

Zhao, Z., L. Lim, et al. (2001). "Blot overlays with 32P-labeled fusion proteins." Methods **24**(3): 194-200.

10. Acknowledgements

I would like to thank:

- Nati Hernando, my thesis supervisor, for her scientific enthusiasm, for the guidance and support through the years of my thesis

- Heini Murer for being my mentor (Doktorvater) and for supporting this work

- Jürg Biber for his continuous interest and for sharing his expertise during my thesis

- Florian Lang, the external member of my thesis committee, for the helpful discussion and advice concerning my project

- All people who contributed with their work to the completion of my thesis: Serge Gisler, Ana Velic, Paola Capuano and Nicole Kampik

- All current and former members of the Murer group for discussions, support and advice

- All J-Floor people for creating a great working atmosphere

- My parents for their great support during all the years of my studies and my thesis

- Josh for his love and especially for his patience with me

Further, I would like to thank:

- Zurich Center for Integrative Human Physiology “ZIHP” for the PhD student fellowship

11. Curriculum vitae

Personal details

Surname	Reining
Forename	Sonja Cornelia
Date of birth	23.01.1980
Place of birth	Dieburg, Deutschland

Education

Since June 2005	PhD student fellowship “Expression and regulation of NaPi-IIa in a murine model deficient for the novel interacting partner GABARAP” Institute of Physiology, Research group Prof. H. Murer and Prof. J. Biber, University of Zurich, Switzerland
June 2004 – Feb. 2005	Diploma thesis “Characterization of the MAPK family member ERK8” Merck KGaA, Department: Target Research and Biotechnology/Target Idendifikation, Darmstadt, Germany
1999 – 2005	Studies of Biology (diploma) Johannes Gutenberg-University, Mainz, Germany
1990 – 1999	Secondary school Dieburg, Germany
1986 – 1990	Primary school Dieburg, Germany

12. Publication

Sonja C. Reining, Serge M. Gisler, Daniel Fuster, Orson W. Moe, Gregory A. O'Sullivan, Heinrich Betz, Jürg Biber, Heini Murer, Nati Hernando

“GABARAP deficiency modulates the expression of NaPi-IIa in renal brush border membranes”

Am J Physiol Renal Physiol. 2009 Feb 18. [Epub ahead of print]